Agricultural Systems 220 (2024) 104066

Contents lists available at ScienceDirect

Agricultural Systems

journal homepage: www.elsevier.com/locate/agsy

Adaptation strategies for winter wheat production at farmer fields under a changing climate: Employing crop and multiple global climate models

Muhammad Rizwan Shoukat [a], Jingjing Wang [a], Muhammad Habib-ur-Rahman [b], Xin Hui [a], Gerrit Hoogenboom [c], Haijun Yan [a,d,*]

[a] College of Water Resources and Civil Engineering, China Agricultural University, Beijing 100083, China
[b] Institute of Crop Science and Resource Conservation (INRES), University Bonn, 53115 Bonn, Germany
[c] Agricultural and Biological Engineering, University of Florida, Gainesville, FL 32611, USA
[d] Engineering Research Center for Agricultural Water-Saving and Water Resources, Ministry of Education, Beijing 100083, China

HIGHLIGHTS

- The GCMs of CMIP6 projected an increase in temperatures and precipitation from 2021–2100, with the peak rise in 2081–2100.
- By 2100, forecasts had predicted a rise in maximum temperatures of 3.19 °C, minimum temperatures of 3.07°C, and precipitation by 23%.
- Increased temperatures, and precipitation variations reduced the winter wheat growing season, grain number and grain yield.
- Adaptation strategies, such as adjusting planting times, optimizing nitrogen use, and enhancing irrigation, positively impacted grain yield.
- Increased CO_2 levels and adaptation strategies can effectively mitigate the adverse warming impacts on grain yields.

GRAPHICAL ABSTRACT

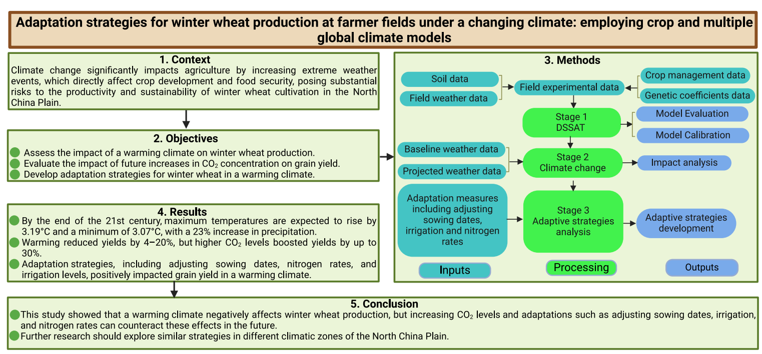

ARTICLE INFO

Editor: Jagadish Timsina

Keywords:
Winter wheat
Adaptation strategies
Climate change
Crop modeling
CMIP6 GCMs
Sustainable wheat production

ABSTRACT

CONTEXT: Climate change profoundly affects agriculture through increased occurrences of extreme weather events, directly affecting crop growth and food security. The North China Plain (NCP), a significant region for winter wheat production, faces challenges from the changing climate, which could threaten agricultural output and sustainability.
OBJECTIVE: This study aimed to evaluate the effects of a warming climate, fluctuating precipitation, and rising CO_2 levels on winter wheat production in the NCP. Additionally, it developed adaptation strategies, such as modifying the timing of planting and adjusting irrigation and nitrogen fertilizer levels, to mitigate the negative impacts of a changing climate on grain production.
METHODS: Using the DSSAT CROPSIM CERES-Wheat and NWheat models, this study incorporated baseline climate data from 2001 to 2020 and future climate projections from 12 GCMs under the CMIP6 framework. The

* Corresponding author.
E-mail address: yanhj@cau.edu.cn (H. Yan).

https://doi.org/10.1016/j.agsy.2024.104066
Received 18 April 2024; Received in revised form 19 June 2024; Accepted 10 July 2024
Available online 26 July 2024

evaluation was segmented into four future terms (terms 1 to 4) spanning from 2021 to 2100, under two societal development scenarios known as Shared Socioeconomic Pathways (SSPs): SSP2–4.5 and SSP5–8.5.
RESULTS AND CONCLUSIONS: The projections indicated an increase in temperature and precipitation over the century, with the most substantial changes under the SSP5–8.5 scenario. Term 1 (2021–2040) forecasts predicted mild temperature increases (0.89 °C increase in average maximum temperature, 0.74 °C in average minimum temperature) and an 8% increase in precipitation. Term 4 (2081–2100) projections indicated a more severe climate impact, with maximum temperatures rising by 3.19 °C, minimum temperatures by 3.07 °C, and seasonal precipitation increasing by 23%. These climatic changes are expected to reduce the winter wheat growing season by 4–17%, decrease grain numbers by 3–21%, and reduce yield by 4–20% compared to the baseline. However, the increase in CO_2 from terms 1 to 4 could enhance grain yield by 4–30% under SSP5–8.5, indicating a complex interaction between climatic factors and crop productivity. This study showed that adaptation strategies, including adjusting planting times (early October), irrigation levels (300–400 mm), and nitrogen fertilizer application (250–300 kg ha^{-1}), can effectively minimize the negative impacts of warming on grain yield.
SIGNIFICANCE: This study underscores the critical need for immediate and effective adaptation strategies to address the impact of climate change on agriculture. By adjusting agricultural practices, the negative effects on winter wheat production in the NCP can be mitigated, thereby contributing to regional food security in the face of ongoing climate challenges.

1. Introduction

Changes in agroclimatic conditions resulting from climate change can pose a substantial risk to worldwide food production (IPCC, 2021; IPCC, 2022; IPCC, 2023), affecting food security. This is particularly true for countries that are susceptible to the impacts of climate change and have a limited ability to adapt to and mitigate its effects. An observed increase of 0.99 °C in global surface temperatures occurred between 2001 and 2020, compared to the period of 1850–1900 (IPCC, 2023). Climate change has a substantial impact on the agricultural industry (Zhang et al., 2023b) and has been the subject of research to forecast its influence on crop output (Zhang et al., 2023a; Ishaque et al., 2023). Climate change can accelerate the growth and maturation of agricultural crops, leading to changes in crop productivity (Lobell and Tebaldi, 2014). The primary factors influencing the impact of climate change on crop production, particularly wheat output in China, are fluctuations in air temperature, precipitation, and CO_2 levels. These factors have substantial ramifications, as highlighted by Wang et al. (2023b).

Winter wheat production in the NCP, the largest alluvial plain, contributes to 53.7% of the overall yield. This region covers approximately 40% of the country's arable territory (Wang et al., 2024a). This area, which is home to China's main economic centre, plays a vital role in wheat cultivation. The NCP has experienced significant changes in temperature and precipitation due to climate change (Wang et al., 2012), which has influenced the development and productivity of winter wheat (Kong et al., 2023). The elevated mean temperature throughout the crop growth period has an adverse impact on the output of winter wheat (Han et al., 2023; Yu et al., 2023). Rising temperatures accelerate growth and developmental phases, shorten the life cycle, impair canopy development, and reduce photosynthesis while increasing respiration rates, ultimately leading to faster development and a shorter grain filling period, crucial for yield accumulation (Liu et al., 2021b; Muleke et al., 2022; Ali et al., 2020; Li and Lei, 2022). Implementing adaptation strategies, such as modifying the timing of planting and enhancing irrigation and fertilizer practices, is essential for mitigating crop production reductions caused by heat stress (Zhang et al., 2023a). Numerous studies have analyzed the impact of climate change on winter wheat by employing cropping system models (CSM) and projecting future climate scenarios in the NCP (Shoukat et al., 2022; Yu et al., 2023).

CSM play a vital role in understanding the impacts of climate change on agricultural production, serving as essential tools that simulate and analyze the complex interactions between crops, soil, climate, and management practices (Asseng et al., 2004; Kassie et al., 2016; Asseng et al., 2015; Wang et al., 2024b) (Summary key features of some CSMs are presented in Table S1). The key models in this subject include DSSAT, APSIM, SWAP, STICS, EPIC, and ORYZA, which serve as the basis for research and analysis (Liu et al., 2021b; Saddique et al., 2020; Hoogenboom et al., 2019; Kassie et al., 2016). Specifically, DSSAT is extensively utilized worldwide to simulate crop growth, productivity, and agricultural practices across several climatic scenarios (Hoogenboom et al., 2019). The CROPSIM-CERES Wheat and NWheat models in DSSAT accurately simulate winter wheat yields in response to varying climatic conditions (Ishaque et al., 2023; Zhang et al., 2023a; Kassie et al., 2016). These models demonstrate the impact of temperature, precipitation, CO_2, and other factors on crop output by considering soil, weather, and agricultural practices. CMIP6 expanded projections offer a comprehensive analysis, allowing for a more profound understanding of vulnerable areas and providing valuable information for the development of adaptive strategies (Zhang et al., 2023a). The improved forecasts derived from CMIP6 provide a deeper understanding of how climate impacts agriculture, highlighting the necessity for resilient adaptation techniques to uphold food security.

Despite significant advances in understanding climate impacts on agriculture, previous studies have primarily relied on older climate projections (CMIP5 and earlier) (Wen et al., 2023; Wang et al., 2023a; Liang et al., 2023), which may not accurately capture current and future climate realities. Moreover, there are a limited number of studies using the latest CMIP6 models to analyze the effects of climate change on winter wheat in the NCP, a critical agricultural region (Zhang et al., 2023a; Jiang et al., 2023). This study introduces a novel approach by utilizing updated CMIP6 multiple GCMs projections and advanced crop system models (DSSAT CROPSIM CERES-Wheat and NWheat) to examine winter wheat phenology, grain numbers, and yields under future climate scenarios (SSP2–4.5 and SSP5–8.5). The application of these updated models allows for a more accurate and detailed assessment of climate impacts on wheat production in the NCP, addressing a significant gap in the literature. By employing the latest CMIP6 models, this study provides more precise forecasts of climate impacts on agriculture, improving upon the limitations of previous studies that have relied on CMIP5 GCMs. We extend the analysis to include both current and future climate scenarios, and evaluated how increased CO_2 emissions and other climatic changes will affect grain yield from 2021 to 2100. This comprehensive approach offers critical insights for developing effective adaptation strategies. Based on our findings, we proposed adaptation measures, including adjusting sowing dates, irrigation, and nitrogen fertilizer levels, to enhance the resilience of winter wheat production in the NCP under a warming climate. These strategies can be tailored to address the adverse warming climate impact on winter wheat and provide actionable guidance for policymakers and agricultural professionals.

Hence, this study utilized the GCMs from CMIP6 to analyze the impact of a warming climate on winter wheat phenology, grain numbers, and grain yield. The study considered both the current climate conditions (baseline) and the projected future climate scenarios of SSP2–4.5 and SSP5–8.5. The main objectives of this study were to measure the effects of a warming climate on winter wheat growth stages (specifically anthesis and maturity days), grain numbers, and grain yield in the NCP using the DSSAT CROPSIM CERES-Wheat and NWheat models. Additionally, this study aimed to assess the impact of projected CO_2 emissions on winter wheat grain yield from 2021 to 2100 under different future climate scenarios. Finally, this study aimed to develop and recommend adaptation strategies to reduce the negative effects of a warming climate on future winter wheat production in the NCP.

2. Materials and methods

2.1. Field experiments for modeling studies

The Zhuozhou Experimental Station of China Agricultural University, located at 39°27′N latitude, 115°5′E longitude, and 42 m above mean sea level in Baoding, Hebei, China, served as the site for field experiments conducted throughout the periods of 2020–2021 and 2021–2022 (Fig. 1). The experimental farm was situated in a semi-humid continental region commonly associated with a temperate monsoon climate zone. The NCP experiences notable variations in precipitation throughout the year, with the majority of the average annual rainfall (550 mm) occurring during the summer season, accounting for 70–80% of the total. Precipitation alone fulfills around 25–40% of the water needs for winter wheat growth in the area. To offset a deficiency in rainfall, it is imperative to provide irrigation water to winter wheat to sustain ideal grain yields. The weather data, which includes the maximum temperature, minimum temperature, and precipitation, were gathered within a 100-m radius of the measurement site using a HOBO U30 automated weather station manufactured by Onset Computer Co., located in Massachusetts, USA (Hui et al., 2022) (Fig. 2). Based on the USDA soil texture triangle, the predominant soil type is sandy. The soil layer from 0 to 40 cm has a maximum accessible water content (AWC) of 0.16 cm^3 cm^{-3}. Prior to wheat sowing, an analysis was conducted to assess the physicochemical properties of the soil. (Table 1).

2.2. Experimental design and treatments

The winter wheat variety Nongda 212 was planted on October 12, 2020, and October 10, 2021, over the course of the two-year experimental period. Winter wheat was sown at a seeding depth of 4 cm, row spacing of 15 cm, and seeding rate of 270 kg ha^{-1}. The experiment was conducted using an irrigation and fertigation system equipped with a center pivot. The trial site encompassed an area of 1.03 ha and employed a three-span center pivot irrigation and fertigation system produced by Modern Agricultural Equipment Co., Ltd., based in Beijing, China. The third span measures 50 m, the overhang extends for 15 m, the first span is 37 m long, the second span measures 38 m, and the center pivot has a length of 140 m (Hui et al., 2022).

The experiment was carried out using a randomized complete block design (RCBD) with three repetitions. Over the course of the two-year winter wheat trials, a total of five different treatments, including the application of nitrogen (N), were conducted. The specifics of these treatments are shown in Table 2. Urea, containing 46% nitrogen, was used as the main nitrogen fertilizer. Throughout the two-year experimental period, nitrogen fertilizer was applied at different stages of growth, specifically during the regreening (169 and 171 days after sowing in the 2020–2021 and 2021–2022 growing seasons, respectively), jointing (195 and 197 days after sowing in the 2020–2021 and 2021–2022 growing seasons, respectively), and anthesis (210 and 211 days after sowing in the 2020–2021 and 2021–2022 growing seasons, respectively) phases. Among the other growth stages, the regreening stage in winter wheat is a crucial phase that occurs after the overwintering stage and before the rising and jointing stages. Throughout the first growth period, 270 mm of irrigation water was provided at

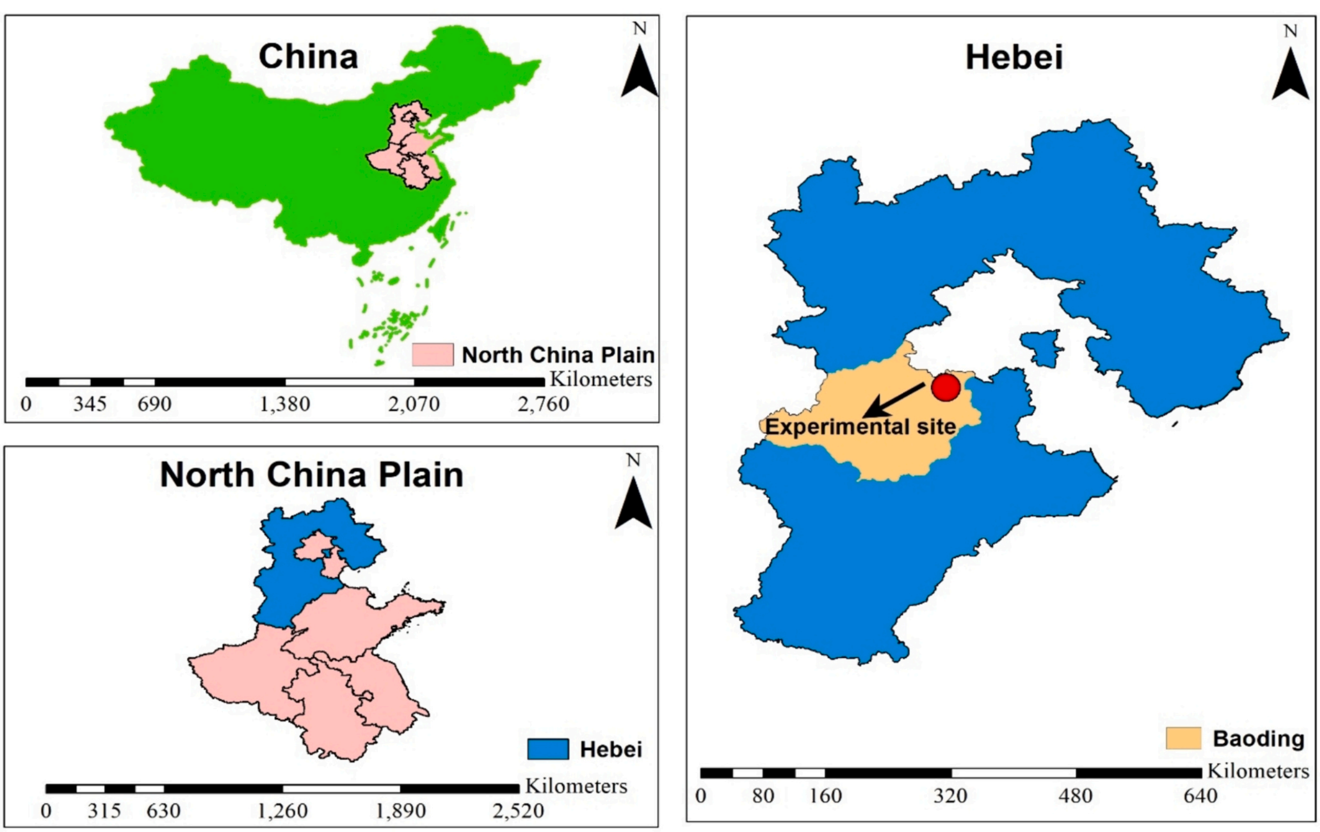

Fig. 1. Experimental site location at the Zhuozhou experimental station of the China Agricultural University, Baoding, Hebei, China.

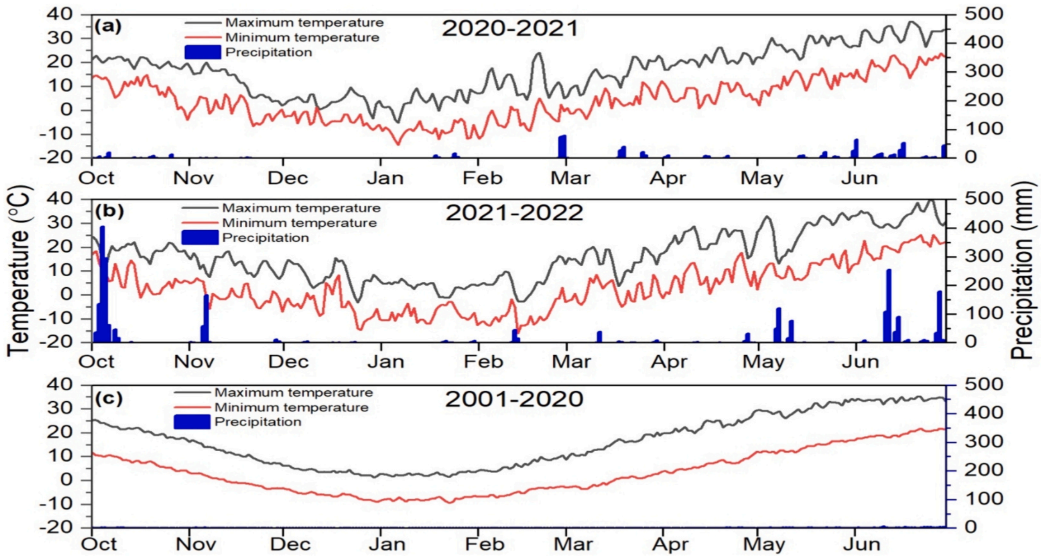

Fig. 2. Maximum temperatures, minimum temperatures, and precipitation during (a) 2020–2021, (b) 2021–2022 wheat growing seasons, and (c) 20 years average monthly baseline.

Table 1
Soil physicochemical properties of the study area used for models' calibration and evaluation.

Depth (cm)	Bulk density (g cm^{-3})	Field capacity (cm^3 cm^{-3})	Available phosphorus (mg kg^{-1})	NH_4^+-N content (mg kg^{-1})	NO_3^-N content (mg kg^{-1})	Potassium (mg kg^{-1})	Organic matter (g kg^{-1})
0–20	1.62	0.24	43.26	7.36	25.59	49.90	11.56
20–40	1.58	0.20	49.35	3.28	9.67	71.08	11.79
40–60	1.57	0.23	19.66	4.64	10.08	57.39	13.14
60–80	1.59	0.16	17.52	2.94	10.71	41.58	10.39

Table 2
Nitrogen fertilizer application at various stages of development of winter wheat throughout the wheat growing seasons (2020−2022).

Treatments	Basal (kg ha^{-1})	Regreening (kg ha^{-1})	Jointing (kg ha^{-1})	Anthesis (kg ha^{-1})	Total N (kg ha^{-1})
N54	54	0	0	0	54
N121	54	30	30	7	121
N187	54	60	60	13	187
N254	54	90	90	20	254
N321	54	120	120	27	321

several stages of development, including overwintering (30 mm), regreening (40 mm), early jointing (30 mm), late jointing (35 mm), heading (30 mm), anthesis (35 mm), early filling (35 mm), and late filling (35 mm). in the second season, irrigation was excluded at the late filling stage due to precipitation. Throughout the crop growth period, further field management activities were carried out in compliance with the established local requirements. In both growing seasons, the crops were harvested on June 7, 2021, and June 8, 2022.

2.3. Crop modeling (calibration, and evaluation)

2.3.1. Description of the DSSAT wheat simulation models

The CSM of the DSSAT is a model that focuses on processes and operates based on mechanisms (Jones et al., 2003). It includes dynamic crop growth simulation models for many types of crops. Recently, additional capabilities have been integrated into DSSAT to enhance its application (Hoogenboom et al., 2023). The present study employed the CROPSIM CERES (CSCER) Wheat (Zhang et al., 2023a) and NWheat models from the latest edition of DSSAT v4.8. The main improvements in the current version involve transitioning to a four-digit year format for the weather files. This shift allows for greater flexibility in simulating historical weather data before 1900, as well as future climate change projections for 2100 and beyond. The defined year in the weather file was selected as the corresponding year for the simulation (Hoogenboom et al., 2023).

Incorporating the CROPSIM CERES-Wheat and NWheat models into the DSSAT version 4.8 framework involved integrating these models into a comprehensive system. Chosen for their effectiveness in climate change and food security research, these models add significant capabilities to the DSSAT, which features multiple modules including soil, Crop template, weather, and a module for managing light and water competition among soil, plants, and atmosphere (Jones et al., 2003). The DSSAT-CERES-Wheat model, created by Ritchie (1985), is particularly noted for its wide use in crop modeling, stemming from innovations by Ritchie and colleagues in the 1970. This model's ability to regulate growth and development through temperature and daylight, coupled with the radiation use efficiency (RUE) technique, enables accurate simulation of both spring and winter wheat phenologies, considering the impact of vernalization (Ritchie, 1985). The incorporation of NWheat into the DSSAT was achieved through modifications to the APSIM-NWheat (Asseng et al., 2004) model by Kassie et al. (2016). The NWheat model was derived from the CROPSIM CERES-Wheat model. The dataset used in the NWheat model was similar to that of CROPSIM CERES-Wheat, but with some differences. These differences include the addition of supplementary cultivar coefficients for calibration (Kheir et al., 2019). Furthermore, this model has been tested globally across diverse agro-climatic and agronomic settings (Kassie et al., 2016; Osman et al., 2020).

2.3.2. Model calibration and evaluation

Calibration is the process of fine-tuning the genetic coefficients for each model and cultivar to precisely reflect the observed outputs in a specified research area (Timsina and Humphreys, 2006). The essential input dataset for model execution consists of local daily meteorological data covering the entire wheat cultivation period, soil physical and chemical data, crop management data, observed data collected during experimental trials, and crop genetic traits (Shoukat et al., 2022).

Model calibration was performed using winter wheat crop data from the second growing season (2021−2022), specifically from a non-stress treatment in which 321 kg ha^{-1} of N fertilizer (N321) was applied, which produced maximum yield compared with the other treatments (Si et al., 2021; Yasin et al., 2022). This data set was selected to establish a robust baseline for the model under optimal growth conditions. To evaluate the model, we used crop data from both the first (2020−2021) and second (2021–2022) growing seasons under various treatments that were not included in the calibration process (Shoukat et al., 2022). This approach ensured that the predictive accuracy of the model was tested against independent datasets, enhancing the validity of the model across different treatment conditions and temporal variations. This dual-phase process ensured that the model could reliably predict winter wheat responses under varying agricultural practices and environmental conditions. NWheat calibration involves manually adjusting the genetic parameters within their known ranges based on genotype data until the values closely match the observed data. On the other hand, CERES-Wheat calibration used trial-and-error with Generalized Likelihood Uncertainty Estimation (GLUE) methods in DSSAT (Ahmed et al., 2016). The genetic parameters of the two calibrated models are listed in Table 3.

Model performance was quantified using the mean absolute percentage error (MAPE), root mean square error (RMSE), normal root mean square error (nRMSE), and Willmott index of agreement (d) (Shoukat et al., 2022).

$$MAPE = \frac{1}{n} \times 100 \times \sum_{i=1}^{n} \left(\frac{Oi - Si}{Oi} \right) \quad (1)$$

$$\mathrm{RMSE} = \sqrt{\frac{1}{\mathrm{n}} \sum_{\mathrm{i}=1}^{\mathrm{n}} (\mathrm{S_i} - \mathrm{O_i})^2} \quad (2)$$

$$\mathrm{nRMSE} = \sqrt{\sum_{i=1}^{n} \frac{(Si - Oi)^2}{n}} \times \frac{100}{\overline{O}} \quad (3)$$

$$\mathrm{d} = 1 - \frac{\sum_{i=1}^{n} (O_i - S_i)^2}{\sum_{i=1}^{n} (|O_i - O| + |S_i - O|)^2} \quad (4)$$

Table 3
Genotypic parameters of cultivar Nongda212 calibrated for the DSSAT CROPSIM CERES-Wheat and NWheat models.

Models	Parameter	Definition	Calibrated value	Default range
CROPSIMCERES-Wheat	PIV	Number of days, the optimal vernalizing temperature (d)	22.63	0–60
	PID	Responses to the photoperiod	90.44	0–200
	P5	Grain-filling stage period (°C d)	500.30	100–999
	G1	At anthesis, the number of kernels per unit canopy weight (kernel weight^{-1})	26.79	10–50
	G2	Size of a standard kernel at optimum conditions (mg)	39.86	10–80
	G3	Weight of mature, non-stressed tillers (g)	1.282	1–8
	PHINT	Leaf tip appearance interval (°C d)	86.00	30–150
	VSEN	Sensitivity to vernalization	1.50	1–4
	PPSEN	Sensitivity to photoperiod	4.00	1–5
NWheat	P1	Thermal time from seedling emergence to the end of the juvenile phase (°Cd)	380.00	380–530
	P5	Thermal time (base 0 °C) from beginning of grain fill to maturity (°Cd)	690.00	200–700
	PHINT	Phyllochron interval	125.00	85–130
	GRNO	Coefficient of kernel number per stem weight at the beginning of grain filling (kernels stem weight^{-1})	32.00	20–32
	MXFIL	Potential kernel growth rate (mg kernel^{-1} day^{-1})	2.90	2–3
	STMMX	Potential final dry weight of a single tiller excluding grain (g stem^{-1})	3.00	1–3
	SLAP1	Ratio of leaf area to mass at emergence (cm^2 g^{-1})	330.00	200–400

2.4. Sixth phase of coupled model intercomparison project

The assessment of climate change is essential for understanding the climate system and addressing socioeconomic hazards and mitigation strategies (O'Neill et al., 2017). The IPCC's Sixth Assessment Report (AR6) highlights the CMIP6 ensemble's potential for exploring climate change mechanisms and improving global climate predictions (IPCC, 2021). The CMIP6 includes the Scenario Model Intercomparison Project (ScenarioMIP), utilizing new simulations based on concentration pathways specified by Tebaldi et al. (2020) to project future climate conditions. This initiative advances General Circulation Models (GCMs) by integrating updated Shared Socioeconomic Pathways (SSPs) and greenhouse gas emission data, enhancing our capability to predict future climatic scenarios (Li et al., 2024; Iqbal et al., 2021). SSPs are vital for addressing impact, vulnerability, adaptation, and mitigation issues. They offer five themes representing various socioeconomic progress pathways, including moderate development, regional competitiveness, disparities, sustainable growth, and fossil fuel reliance (Riahi et al., 2017). These scenarios, particularly SSP2–4.5 and SSP5–8.5, are crucial for assessing climate impacts and adaptations. The selection of SSP2–4.5 and SSP5–8.5 scenarios for this study offers insights into a broad spectrum of potential futures. SSP2–4.5, the "middle-of-the-road" scenario, focuses on sustainability with moderate socioeconomic development and reduced emissions, ideal for evaluating balanced growth and environmental strategies. SSP5–8.5, the "business-as-usual" scenario, reflects a high-growth trajectory with minimal mitigation efforts, crucial for assessing the upper limits of climate impacts. These scenarios enable a thorough analysis of climate risks and adaptation measures across different development paths (O'Neill et al., 2017). These scenarios enable researchers to evaluate the effects of climate change and the necessary adaptive measures under different levels of socioeconomic development and environmental change (O'Neill et al., 2020).

2.5. Global climate models and statistical downscaling

The China Meteorological Data Sharing Service System (CMDSSS) (http://cdc.cma.gov.cn, retrieved on November 5, 2022) provided historical meteorological data for a period of 20 years that including daily precipitation, solar radiation, and maximum and minimum air temperatures (Li et al., 2023). The World Climate Research Programme (WCRP) and Earth System Grid Federation (ESGF) websites (https://esgf-node.llnl.gov/search/cmip6/, retrieved on November 10, 2022) were used to obtain the 12 GCMs' raw climate data for maximum temperature, minimum temperature, and precipitation for the years 2021–2100 under the SSP2–4.5 and SSP5–8.5 scenarios (Shoukat et al., 2022; Zhang et al., 2023a). The same datasets were downloaded using the same 'r1i1p1f1' variant (first realization, first initialization, first physics, and first forcing). The selection of these 12 GCMs was based on their climatological characteristics as well as their representation of different regions (Gul et al., 2020) (Table 4). The climatic data from 12 GCMs, specifically pertaining to maximum and minimum temperatures as well as precipitation, were analyzed under two different scenarios: SSP2–4.5 and SSP5–8.5. These scenarios are further divided into four distinct terms:1 (2021–2040), 2 (2041–2060), 3 (2061–2080), and 4 (2081–2100). The purpose of this analysis was to assess the impact of climate change on these four terms.

Ashfaq et al. (2022) found that although some CMIP6 GCMs have a horizontal grid spacing of half a degree, most of them do not have the required resolution (>1° horizontal grid spacing) to adequately assess regional and local-scale mitigation and adaptation solutions. Therefore, it is crucial to utilize downscaling techniques to improve the geographical resolution of anticipated climate change data. Statistical downscaling approaches are frequently used to obtain precise regional data at a more refined scale (Ur Rahman et al., 2018). Statistical downscaling involves the examination of large-scale atmospheric factors, such as circulation patterns, in connection with climatic surface variables (Salehnia et al., 2019). Downscaling can be used to bridge the gap between climatic outputs and the data requirements of different agricultural and hydrological models. This approach enables the evaluation of the impact of climate change on crop productivity and food security at local and site-specific levels. The study utilized the SD-GCM v2.0 (Statistical Downscaling of General Circulation Models) software (Shoukat et al., 2022; Salehnia et al., 2019). The software permitted the downscaling of CMIP6 model climate data on a daily, monthly, or yearly basis under SSP scenarios, making it highly valuable for its application. In our investigation, we utilized the delta method for statistical downscaling, which is a commonly used approach for downscaling GCM outputs. Owing to its straightforward implementation and intrinsic comprehensibility, this strategy is often recognized as the most efficient.

Table 4
CMIP6 GCMs were used to project future climates under the SSP2–4.5- and SSP5–8.5-scenarios.

Code	GCM	Institute	Variant label	Lon. × Lat.
1	ACCESS-CM2	Commonwealth Scientific and Industrial Research Organization, Australia	r1i1p1f1	192° × 144°
2	CanESM5	Canadian Centre for Climate Modeling and Analysis, Canada	r1i1p1f1	128° × 64°
3	EC-Earth3	European EC-Earth consortium	r1i1p1f1	512° × 256°
4	GFDL-CM4	Geophysical Fluid Dynamics Laboratory, USA	r1i1p1f1	144° × 90°
5	GFDL-ESM4	Geophysical Fluid Dynamics Laboratory, USA	r1i1p1f1	288° × 180°
6	INM-CM5–0	Institute for Numerical Mathematics, Russia	r1i1p1f1	180° × 120°
7	IPSL-CM6A-LR	Institute Pierre Simon Laplace, France	r1i1p1f1	144° × 143°
8	MIROC6	Japan Agency for Marine-Earth Science and Technology, Japan	r1i1p1f1	256° × 128°
9	MPI-ESM1–2-LR	Max Planck Institute for Meteorology, Germany	r1i1p1f1	192° × 96°
10	MRI-ESM2–0	Meteorological Research Institute, Tsukuba, Japan	r1i1p1f1	320° × 160°
11	NorESM2-LM	Norwegian Climate Centre, Norway	r1i1p1f1	144° × 96°
12	TaiESM1	Research Center for Environmental Changes, Academia Sinica, Taiwan	r1i1p1f1	288°x192°

2.6. Projections of climate change impact on winter wheat production

After calibrating and validating the models, we used the calibrated DSSAT CROPSIM CERES-Wheat and NWheat models to simulate the phenology of winter wheat, including the number of days to anthesis and maturity, grain number, and grain yield (Zhang et al., 2023a). The calibration treatment, encompassing all management practices, such as sowing, fertilization, and irrigation, was utilized to assess the impact of climate change (Yasin et al., 2022). This was accomplished by employing the reference period (2001−2020) and analyzing future meteorological data (maximum and minimum temperature and precipitation) from 12 GCMs under the SSP2–4.5 and SSP5–8.5 scenarios. An investigation was conducted to analyze the phenology, grain numbers, and grain yield of winter wheat in the NCP across four successive periods: Term 1 (2021–2040), Term 2 (2041–2060), Term 3 (2061–2080), and Term 4 (2081–2100). This investigation employed the DSSAT CROPSIM CERES-Wheat and NWheat models in seasonal analysis tools. The current study examined the expected patterns of daily maximum and minimum temperature and precipitation, specifically within the framework of the SSP2–4.5 and SSP5–8.5 scenarios. It was presumed that all the other climatic factors remained consistent. Other researchers have utilized similar approaches in their investigations (Ur Rahman et al., 2018; Yasin et al., 2022). The CERES-Wheat and NWheat models were used to create weather datasets using daily historical climate data from 2001 to 2020. In addition, we used daily climate data projections from the GCMs for the SSP2–4.5 and SSP5–8.5 scenarios. These projections were used for four specific time periods, referred to as terms 1, 2, 3, and 4.

The equation employed in this study assesses the impact of climate variability on winter wheat yield (Ur Rahman et al., 2018).

$$\Delta Y = \left(\frac{Si - Oi}{Oi}\right) \times 100 \tag{5}$$

In the given equation, ΔY represents the alteration in grain yield, Si denotes the mean anticipated yield in the future, and Oi is the mean yield during the baseline period.

2.7. Projected CO_2 concentrations impact on winter wheat grain yield

The CO_2 concentrations projected under the SSP2–4.5 scenario were 460, 522, 575, and 601 ppm for terms 1, 2, 3, and 4, respectively, according to IPCC-AR6 (IPCC, 2021). Similarly, the CO_2 concentrations associated with the SSP5–8.5 scenario were 476, 603, 804, and 1067 ppm for the same terms. These projections were subsequently modified using the environmental modification seasonal analysis tool of the calibrated CROPSIM CERES-Wheat and NWheat models. The EC-Earth3 GCM was chosen to assess the influence of CO_2 on the winter wheat grain yield. It demonstrated the highest level of agreement with other GCMs in terms of increasing maximum and minimum temperatures, as well as precipitation, as a comparable methodology was employed by ur Rahman et al. (2018). The baseline climate data for the current study comprised historical climate data from 2001 to 2020. The DSSAT model considers a default CO_2 concentration of 380 ppm as the baseline level. Multiple studies have utilized similar approaches to investigate the impact of CO_2 concentrations on crop productivity within representative concentration pathway (RCPs) scenarios (Ur Rahman et al., 2018). The study evaluated winter wheat grain production under the SSP2–4.5 and SSP5–8.5 scenarios, which are based on different CO_2 concentrations, with the baseline CO_2 concentration.

2.8. Sensitivity analysis to temperature changes and exploring adaptive management scenarios in a warming climate

The sensitivity analysis of winter wheat production to temperature changes was conducted using the DSSAT CROPSIM-CERES Wheat and NWheat models, incorporating an environmental modification tool (Ishaque et al., 2023). The baseline climate data from 2001 to 2020 served as the foundation for this analysis. Calibration treatments, which included comprehensive management practices such as sowing, fertilization, and irrigation, were applied to assess the impact of temperature variations on winter wheat production. We adjusted the maximum and minimum temperatures in increments of 1, 2, 3, and 4 °C using the environmental modification tool in both models. Four distinct treatments, ranging from 1 °C to 4 °C, were designed to evaluate the sensitivity of winter wheat to each incremental increase in baseline temperature. This methodology mirrors the approaches used in previous studies to assess the effects of increasing temperatures on crop production (e.g., Ur Rahman et al., 2018; Ahmad et al., 2020).

This study explored adaptation strategies to mitigate the adverse effects of warming climate on winter wheat grain yield for the period 2021 to 2040, using the well-calibrated DSSAT CROPSIM-CERES Wheat and NWheat models (Ur Rahman et al., 2018; Yasin et al., 2022). The analysis utilized a 20-year dataset from the Term 1 of the EC-Earth3 GCM under SSP2–4.5 and SSP5–8.5 scenarios. This study assessed the impact of different sowing dates, N fertilizer rates, and irrigation levels under Term 1 on winter wheat grain yield. Various irrigation levels (0, 100, 200, 300, 400, and 500 mm) and N fertilizer rates (0, 50, 100, 150, 200, 250, 300, 350, and 400 kg ha^{-1}) were assessed, along with a range of sowing dates from September 24 to November 12, spaced weekly. This included analyzing the optimal sowing date of early October, as recommended for the NCP region (Wang et al., 2012). Winter wheat sowing in early October and application of 300 mm irrigation and 300 kg ha^{-1} N fertilizer were considered traditional practices in the NCP (Jia et al., 2014; Fang et al., 2010; Wang et al., 2012). Irrigation water was utilized at various developmental stages, including overwintering, regreening, early jointing, late jointing, heading, anthesis, and early filling stages. The initial dose of N fertilizer was placed as the basal dose, while the remaining N fertilizer was later added as a top dressing at various growth stages, such as regreening, jointing, and anthesis. The grain yield was then compared under various irrigation levels, nitrogen fertilizer rates, and sowing dates. Based on the observed maximum grain yield, optimal adaptation strategies are suggested for a warmer climate.

3. Results

3.1. DSSAT CROPSIM CERES-Wheat and NWheat calibration and evaluation

The DSSAT CROPSIM CERES-Wheat and NWheat models were calibrated using a minimal-stress-based optimal treatment (N321). This treatment resulted in higher grain yield during the wheat growing season of 2021–2022. The genetic coefficients of both DSSAT models were computed in order to align the simulated and observed data. The calculated genetic coefficients for PIV, PID, P5, G1, G2, G3, and PHINT in the CROPSIM CERES-Wheat model were 22.63, 130.0, 500.3, 26.79, 39.86, 1.282, and 86, respectively (Table 3). In the calibration phase, the simulated anthesis date exhibited a good match with the real data, resulting in an MAPE of zero. Table 3 presents the estimated genetic coefficients for VSEN, PPSEN, P1, P5, PHINT, GRNO, MXFIL, STMMX, and SLAP1 in the DSSAT NWheat model. The respective values for these coefficients are 1.50, 4.0, 380.0, 690.0, 125.0, 32.0, 2.90, 3.0, and 333.0. The results obtained from calibrating the model demonstrated its effectiveness in accurately reproducing phenology, grain number, and grain yield. The MAPE values for the comparison between the simulated and observed anthesis days, maturity days, grain numbers, and grain yield were 0.00%, −0.40%, 6.60%, and −4.30%, respectively, as reported in the CROPSIM CERES-Wheat model (Table S2). The MAPE values for anthesis days, maturity days, grain counts, and grain yield in NWheat were 2.40%, 1.70%, 9.0%, and 4.60%, respectively (Table S3), when comparing the simulated and observed data. These findings indicate that the calibration of the CROPSIM CERES-Wheat model exhibited superior reliability compared to NWheat, as evidenced by the lower MAPE.

The evaluation of the calibrated DSSAT CROPSIM CERES-Wheat and NWheat models was conducted using field data from the remaining treatments in both years of the experiment. These treatments were not included in the calibration process and performance of the both models evaluation is presented below.

3.1.1. Evaluation of CROPSIM CERES-Wheat and NWheat models for nitrogen effects on winter wheat

The performance of the models was assessed based on anthesis days (AD), maturity days (MD), grain number (GN), and grain yield (GY) using RMSE, nRMSE, and d (Table S4). For the CROPSIM CERES-Wheat model, the RMSE values for AD, MD, GN, and GY during the 2020–2021 season were 1 day, 2.00 days, 1338 m^{-2}, and 402 kg ha^{-1}, respectively, with nRMSE of 0.50% for AD, 0.80% for MD, 8% for GN, and 7% for GY, and d values of 0.96 for GN and 0.97 for GY. In the 2021–2022 season, the RMSE values were 0 for AD, 1 for MD, 1420 m^{-2} for GN, and 399 kg ha^{-1} for GY, with corresponding nRMSE of 0 for AD, 0.40% for MD, 7% for GN, and 6% for GY, and d values of 0.96 for GN and 0.97 for GY. For the NWheat model, the 2020–2021 RMSE values were 6 days for AD, 4 days for MD, 1641 m^{-2} for GN, and 526 kg ha^{-1} for GY, with nRMSE of 2.90% for AD, 1.70% for MD, 10% for GN, and 9% for GY, and d values of 0.93 for GN and 0.95 for GY. In the 2021–2022 season, the RMSE values were 5 for AD, 4 for MD, 1830 m^{-2} for GN, and 410 kg ha^{-1} for GY, with nRMSE of 2.40% for AD, 1.70% for MD, 9% for GN, and 9% for GY, and d values of 0.93 for GN and 0.97 for GY. These results indicate that both models performed well in simulating crop phenology, grain number, and grain yield, with generally low RMSE and nRMSE values and high d values, though CERES-Wheat showed slightly better accuracy and agreement compared to NWheat.

3.2. Projected warming climate and precipitation

3.2.1. Baseline and overview of projections

The average maximum and minimum temperatures during the baseline period (2001–2020) were 14.20 °C and 1.07 °C, respectively. The average seasonal precipitation was 160 mm. The multi-GCM ensemble forecasted a rise in both the average seasonal maximum and minimum temperatures, as well as a slight increase in precipitation, for the winter wheat-growing period in Term 1, Term 2, Term 3, and Term 4 under the SSP2–4.5 and SSP5–8.5 scenarios compared to the baseline period (Tables S5, S6, S7, and S8).

3.2.2. Projections on maximum temperatures

All GCMs showed identical estimates for the average increase in maximum temperature (Tmax) across periods 1, 2, 3, and 4, as shown in Table S5. The study found that SSP2–4.5 had the smallest increase in the average ensemble Tmax, whereas SSP5–8.5 observed the largest elevation in Tmax. The GCMs in term 4 indicated a more significant predicted increase in Tmax compared to the other terms, whereas the GCMs in term 1 projected the least rise in Tmax. TaiESM1 exhibited the most significant increase in Tmax, reaching a maximum of 4.13 °C during the Term 4. On the other hand, CanESM5 and MIROC6 projected the smallest increase in Tmax, with a value of 0.10 °C during the Term 1 and Term 2, respectively, under the SSP2–4.5 scenario when compared to the baseline period. According to the SSP5–8.5 scenario, the TaiESM1 anticipated the largest increase in Tmax, reaching a maximum of 6.93 °C in term 4. On the other hand, the MIROC6 model projected the lowest increase in maximum temperature, with only 0.10 °C compared to the baseline period (Table S5).

3.2.3. Projections on minimum temperatures

All GCMs showed identical estimates for the average increase in minimum temperature (Tmin) across periods 1, 2, 3, and 4 (Table S6). The SSP2–4.5 scenario showed the lowest observed increase in the average ensemble Tmin, whereas the SSP5–8.5 scenario displayed the highest recorded increase in Tmin. The GCMs in term 4 forecasted a greater rise in Tmin compared to the previous terms, whereas term 1 anticipated the smallest increase in Tmin. ACCESS-CM2 exhibited the most significant increase in Tmin, reaching a maximum of 3.25 °C during Term 4, while INM-CM5–0 projected the smallest increase in Tmin of 0.05 °C during Term 1 under the SSP2–4.5 scenario, in comparison to the baseline period. According to the SSP5–8.5 scenario, the CanESM5 model anticipated the biggest increase in Tmin, reaching a maximum of 6.87 °C during Term 4. On the other hand, the IPSL-CM6A-LR model projected the lowest increase in Tmin, with only 0.40 °C compared to the baseline period (2001–2020) (Table S6).

3.2.4. Projections on precipitation

The majority of the GCMs predicted an increase in precipitation, with the exception of EC-Earth3 and TaiESM1 (Table S8). The SSP2–4.5 scenario exhibited the smallest increase in average ensemble precipitation, whereas SSP5–8.5 scenario demonstrated the highest increase in precipitation. MRI-ESM2–0 exhibited the most significant increase in precipitation, reaching a peak of 71.83% during Term 4. Conversely, EC-Earth3 projected a decrease in precipitation of 38.81% during Term 1 under the SSP2–4.5 scenario relative to the baseline period. According to the SSP5–8.5 scenario, the MRI-ESM2–0 model expected the largest rise in precipitation, reaching a maximum of 77.20% during Term 4. In contrast, the IPSL-CM6A-LR model projected a decrease in precipitation of 19.65% compared to the baseline period. During the Term 4, it is expected that there will be a significant rise in the average maximum temperature, minimum temperature, and precipitation during the winter wheat growing season.

3.3. Projected warming climate and precipitation impact on crop phenology

The DSSAT CROPSIM CERES-Wheat model projected a mean duration of 211 days from sowing to anthesis and 239 days from sowing to physiological maturity for winter wheat in the baseline simulations (Figs. S1 and S3). On the other hand, the NWheat model calculated the durations to be 212 and 240 days, respectively, as shown in Figs. S2 and S4. Both DSSAT models showed a decrease in the anthesis and physiological maturity days relative to baseline. The decrease was not as significant in the Term 1 but became more substantial in the Term 4. The CROPSIM CERES-Wheat and NWheat models indicated a drop of 6 and 5 days in anthesis, respectively, and a decrease of 6 days in maturity days during Term 1 compared to the baseline period. During Term 2, the CROPSIM CERES-Wheat and NWheat models predicted a decrease of 9 and 8 days, respectively, in each anthesis maturity stage. During Term 3, the CROPSIM CERES-Wheat and NWheat models predicted a decrease of 11 and 9 days, respectively, in the anthesis stage, and a decrease of 12 and 11 days, respectively, in maturity stage, compared to the baseline period. In Term 4, the CROPSIM CERES-Wheat and NWheat models projected a reduction of 13 and 11 days, respectively, in the anthesis stage, and a reduction of 13 and 16 days, respectively, in the maturity stage. Compared with the SSP2–4.5 scenario, the SSP5–8.5 scenario exhibited the greatest reduction in anthesis and maturity days. This was attributed to a significant increase in temperature relative to the baseline period. Under the SSP5–8.5 scenario, both DSSAT models predicted a decrease of 10–12 days in anthesis and 12–13 days in maturity compared to the baseline period. Under the SSP2–4.5 scenario, there was a decrease of 8–9 days in the duration of anthesis, and maturity days. Based on these findings, it is likely that climate change will have a substantial impact on the flowering and maturity stages of winter wheat in the future.

3.4. Projected warming climate and precipitation impact on grain numbers

During the baseline period from 2001 to 2020, the average grain numbers simulated by CROPSIM CERES-Wheat and NWheat were 23,674 m^{-2} and 22,379 m^{-2}, respectively (Figs. 3 and 4). A thorough analysis utilizing an average of 12 GCMs demonstrated a widespread decrease in the average number of grains compared to the baseline period except CanESM5 GCM. The CERES-Wheat model, when paired with the CanESM5 GCM, predicted a 1.82% increase in grain numbers for Term 1 (2021–2040) under the SSP2–4.5 scenario, and a 1.27% increase under the SSP5–8.5 scenario. In contrast, when NWheat was combined with the same GCM, it resulted in a projected increase of 3.18% and 2.30% in grain numbers under the aforementioned scenarios, respectively.

Term 4 exhibited notable decreases in grain numbers, reaching 28% and 25% according to the projections of CROPSIM CERES-Wheat and NWheat, respectively, when applying the TaiESM1 GCM under the SSP2–4.5 scenario. This substantial decline corresponds to the anticipated rise in both the upper and lower temperatures, as well as a 22% decrease in precipitation, according to the projections of the TaiESM1 GCM. According to the CROPSIM CERES-Wheat and NWheat models, under the more extreme SSP5–8.5 scenario, grain numbers are anticipated to decrease by 54% and 43%, respectively, for Term 4 with the CanESM5 GCM. These estimates were accompanied by significant increases in both the maximum and minimum temperatures, as well as a 57% increase in rainfall compared to the baseline period. Each term exhibited different levels of decrease in grain number, which corresponded to gradual changes in the environmental variables. The overall reduction in grain numbers projected by CROPSIM CERES-Wheat and NWheat varies from 3 to 7%, 7 to 11%, 10 to 15%, and 16 to 21% for Term 1, 2, 3, and 4 respectively. Overall, Terms 1 through 4, a comprehensive analysis incorporating CERES-Wheat and NWheat, coupled with the 12 GCMs, revealed a noticeable decrease in average grain numbers, ranging from 3 to 21%.

3.5. Projected warming climate and precipitation impact on grain yield

The DSSAT CROPSIM CERES-Wheat and NWheat models simulated an average wheat grain production of 8668 kg ha^{-1} and 8433 kg ha^{-1}, respectively, throughout the baseline period from 2001 to 2020. The average grain yield, as indicated by the ensemble mean of the 12 GCMs, showed a consistent decrease compared to the baseline. This pattern is illustrated in Figs. 5 and 6. Overall GCMs projections showed a decrease in grain yield with increasing temperature and precipitation in all terms under SSP2–4.5 and SSP5–8.5 scenarios except CanESM5 GCM projection in Term 1. During Term 1 (2021–2040), the combination of the CROPSIM CERES-Wheat model and the CanESM5 GCM forecasted a 1.32% increase in grain yield under the SSP2–4.5 scenario and a 0.16% increase under the SSP5–8.5 scenario. In contrast, the NWheat model, using the same GCM, predicted a 2.89% and 1.82% rise in winter wheat grain yield under the demonstrated conditions due to a slight increase in maximum and minimum temperatures and rise in precipitation (Tables S5, S6, and S8). Term 4 indicated a substantial decrease in yield, with declines of up to 23% and 21% under the SSP2–4.5 scenario, as projected by the CROPSIM CERES-Wheat and NWheat models, respectively due to a higher rise in maximum and minimum temperatures and increase in precipitation. More severe impacts are projected under the SSP5–8.5 scenario, where grain yield reductions of 50% and 42% are

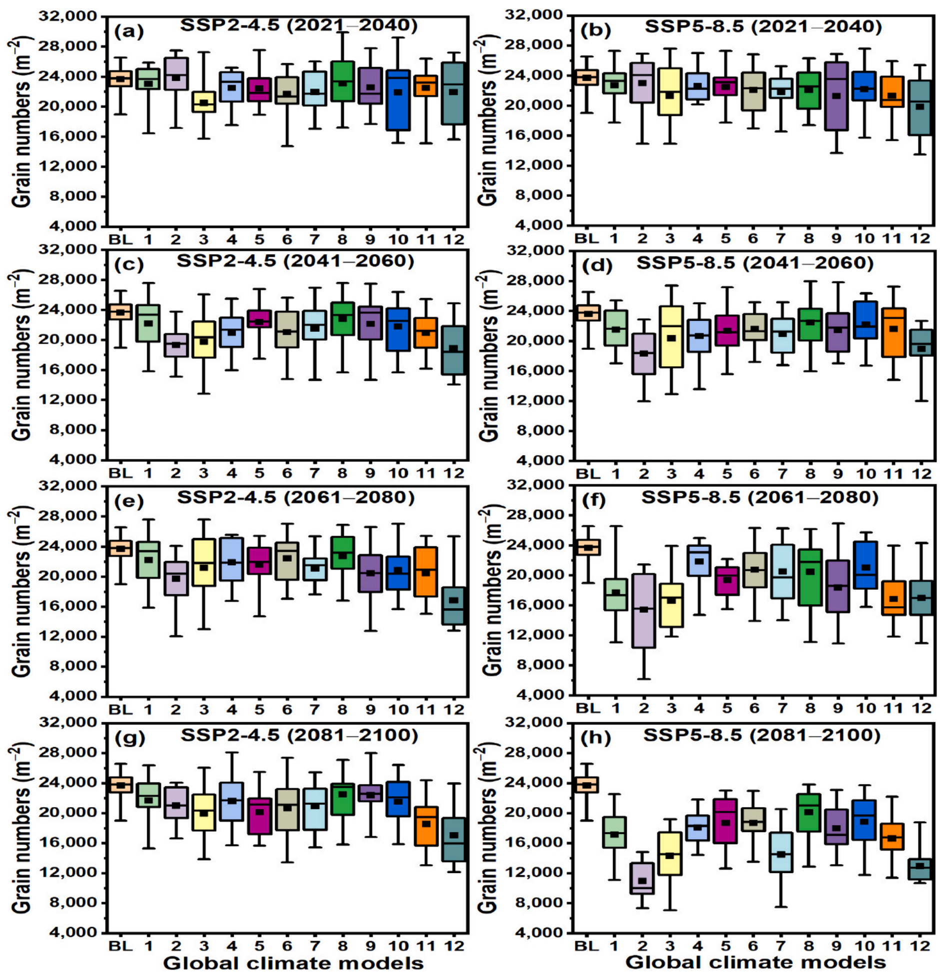

Fig. 3. CROPSIM CERES-Wheat projected warming climate and precipitation impact on winter wheat grain numbers in Term 1, 2, 3, and 4 under SSP2–4.5 (a,c,e, and g) and SSP5–8.5 (b,d,f, and h) scenarios. Where BL represents the baseline, and 1 (ACCESS-CM2), 2 (CanESM5), 3 (EC-Earth3), 4 (GFDL-CM4), 5 (GFDL-ESM4), 6 (INM-CM5–0), 7 (IPSL-CM6A-LR), 8 (MIROC6), 9 (MPI-ESM1.2-LR), 10 (MRI-ESM2–0), 11 (NorESM2-LM), and 12 (TaiESM1) represent GCMs.

forecasted by the CROPSIM CERES-Wheat and NWheat models, respectively. Based on the CanESM5 GCM, this period is projected to have a significant increase in maximum temperature of 5.29 °C, a rise in minimum temperature of 6.87 °C, and a 57% increase in precipitation compared to the baseline period.

Term 1 was anticipated to have the lowest decrease in average grain yield, with reductions ranging from 4% to 5%. The overall GCMs forecasts indicated a 0.89 °C increase in seasonal average maximum temperature, a 0.74 °C increase in average minimum temperature, and an 8% increase in average precipitation compared to the baseline period. However, as the terms progress, the impact intensifies with a predicted decrease of 6–9% in Term 2 and 8–14% in Term 3. This decrease is projected to be due to increase in maximum (1.65 °C and 2.41 °C in Term 2 and Term 3 respectively) and minimum temperatures (1.49 °C and 2.29 °C in Term 2 and Term 3 respectively), as well as more precipitation (13% and 19% in Term 2 and Term 3 respectively). Term 4 is expected to have a decrease in yield of 14–19%, along with an increase in average maximum temperature of 3.19 °C, a rise in average minimum temperature of 3.07 °C, and a 23% increase in average precipitation. Projections from both the CROPSIM CERES-Wheat and NWheat models, when combined with multiple climate models, showed an average decrease in yield ranging from 4 to 20% for the winter wheat seasons from 2021 to 2100. These results underscore the pressing need to implement robust adaptive strategies to counter the adverse impacts of climate change on winter wheat production.

3.6. Effect of CO_2 concentrations scenarios on future winter wheat grain yield

The CROPSIM CERES-Wheat and NWheat models projected the increase in winter wheat grain yield with increasing future CO_2 concentrations compared to a baseline CO_2 concentration of 380 ppm under the SSP2–4.5 and SSP5–8.5 scenarios of EC-Earth3 GCM (Figs. 7 and 8). Under the SSP2–4.5 scenario, our projections using the CROPSIM CERES-Wheat and NWheat models showed grain yields ranging from 7731 to 7768 kg ha^{-1} in Term 1, gradually decreasing to 7551 to 7593 kg ha^{-1} by Term 4 with baseline CO_2 concentration. In stark contrast, under the SSP5–8.5 scenario, initial yields were similar (7721 to 7742 kg ha^{-1} in Term 1) but showed a more pronounced decline, reaching as low as 5594 to 5606 kg ha^{-1} in Term 4. However future expected increased CO_2 concentrations from 460 to 1067 ppm showed a positive impact on winter wheat grain yield under both scenarios across all terms. The most significant yield increase was observed in Term 4 under the SSP5–8.5 scenario, where CO_2 concentrations peaked at 1067 ppm, resulting in a 30% increase in yield relative to the baseline. Conversely, under the SSP2–4.5 scenario with a CO_2 concentration of 601 ppm, the models predicted a modest 12% yield increase. The smallest increase, only 4%, occurred under the SSP2–4.5 scenario at a CO_2 concentration of 460 ppm. These findings indicate that in this specific situation, even a slight rise in CO_2 levels resulted in a smaller increase in grain production. Overall, our models suggested that grain yields could increase by 4% to 30% as CO_2 concentrations rise from 460 ppm to 1067 ppm under

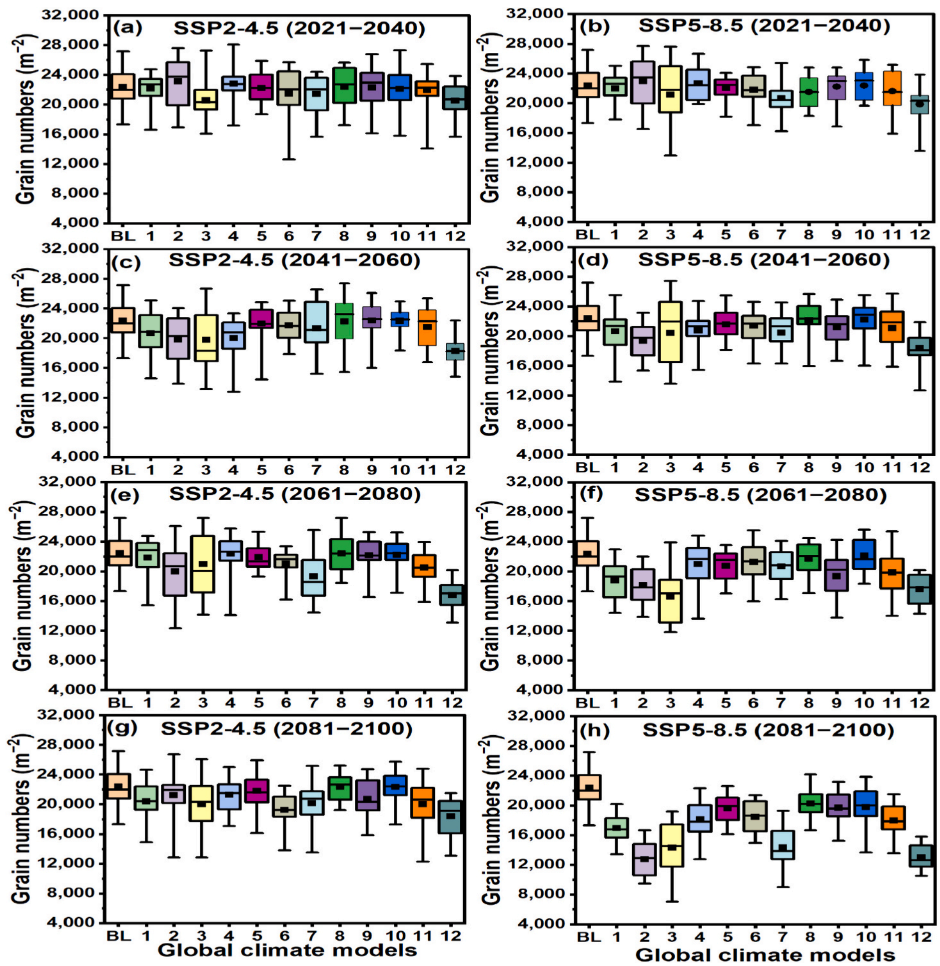

Fig. 4. DSSAT NWheat projected warming climate and precipitation impact on winter wheat grain numbers in Term 1, 2, 3, and 4 under SSP2–4.5 (a,c,e, and g) and SSP5–8.5 (b,d,f, and h) scenarios. Where BL represents the baseline, and 1 (ACCESS-CM2), 2 (CanESM5), 3 (EC-Earth3), 4 (GFDL-CM4), 5 (GFDL-ESM4), 6 (INM-CM5–0), 7 (IPSL-CM6A-LR), 8 (MIROC6), 9 (MPI-ESM1.2-LR), 10 (MRI-ESM2–0), 11 (NorESM2-LM), and 12 (TaiESM1) represent GCMs.

the SSP5–8.5 scenario compared to the baseline concentration in a warming climate. This analysis demonstrated the substantial potential influence of increasing atmospheric CO_2 levels on the winter wheat grain yield in a future warming climate.

3.7. Winter wheat sensitivity to temperature changes and adaptation strategies in a warming climate

3.7.1. Winter wheat sensitivity to temperature changes

This study evaluated the temperature sensitivity of wheat grain production using NWheat and CROPSIM CERES-Wheat models. At the present baseline temperatures, the NWheat model predicted an average yield of 8433 kg ha^{-1}, whereas the CROPSIM CERES-Wheat model predicted a slightly higher average yield of 8668 kg ha^{-1}. When subjected to higher temperatures, both models exhibited a decrease in the yield response (Fig. 9a and b). However, the extent and rate of the decrease differed among the models. Specifically, as temperatures increased from 1 °C to 4 °C above the baseline, yield reductions varied significantly: the models projected a milder decrease of 13% to 16% at a 1 °C increase, escalating to a more pronounced decrease of 42% to 44% at a 4 °C increase. These findings highlight the profound impact of temperature variations on winter wheat yields and illustrate the varying degrees of sensitivity between the two models under thermal stress and the necessity for resilient adaptive strategies, such as modifying sowing dates, adjusting nitrogen fertilizer, and irrigation practices in a warming climate.

3.7.2. Adaptive sowing timing for optimal winter wheat production under warming climate

The current study utilized the DSSAT CROPSIM-CERES Wheat and NWheat models to evaluate the appropriate planting dates for winter wheat in the face of changing climatic conditions. We incorporated climate projections from the EC-Earth3 GCM, specifically under the SSP scenarios SSP2–4.5 and SSP5–8.5 (Fig. 10). The study showed that planting on October 1st produced the highest average grain yield. Under SSP2–4.5, the yield was 7859 kg ha^{-1} (CROPSIM CERES-Wheat) and 7903 kg ha^{-1} (NWheat). Under SSP5–8.5, the yield was 7751 kg ha^{-1} (CROPSIM CERES-Wheat) and 7859 kg ha^{-1} (NWheat). A progressive decline in grain yield was noted for sowing dates deviating from October 1st, either earlier or later. A notable decrease was observed with a slight delay in sowing: yields dropped by 1% when sowing was postponed to October 8th. More significant reductions were recorded with earlier sowing on September 24th, leading to a 6% yield reduction under both SSP2–4.5 and SSP5–8.5 scenarios. The most substantial decline occurred with delayed sowing to November 12th, where yields decreased by up to 16%. These findings emphasize the critical importance of the early October sowing window, particularly around the first week, to maximize grain production under changing climate conditions.

3.7.3. Adaptive nitrogen management for enhanced grain yield under warming climate

Our analysis utilized the DSSAT CROPSIM-CERES Wheat and NWheat models to estimate the most suitable amount of N fertilizer for

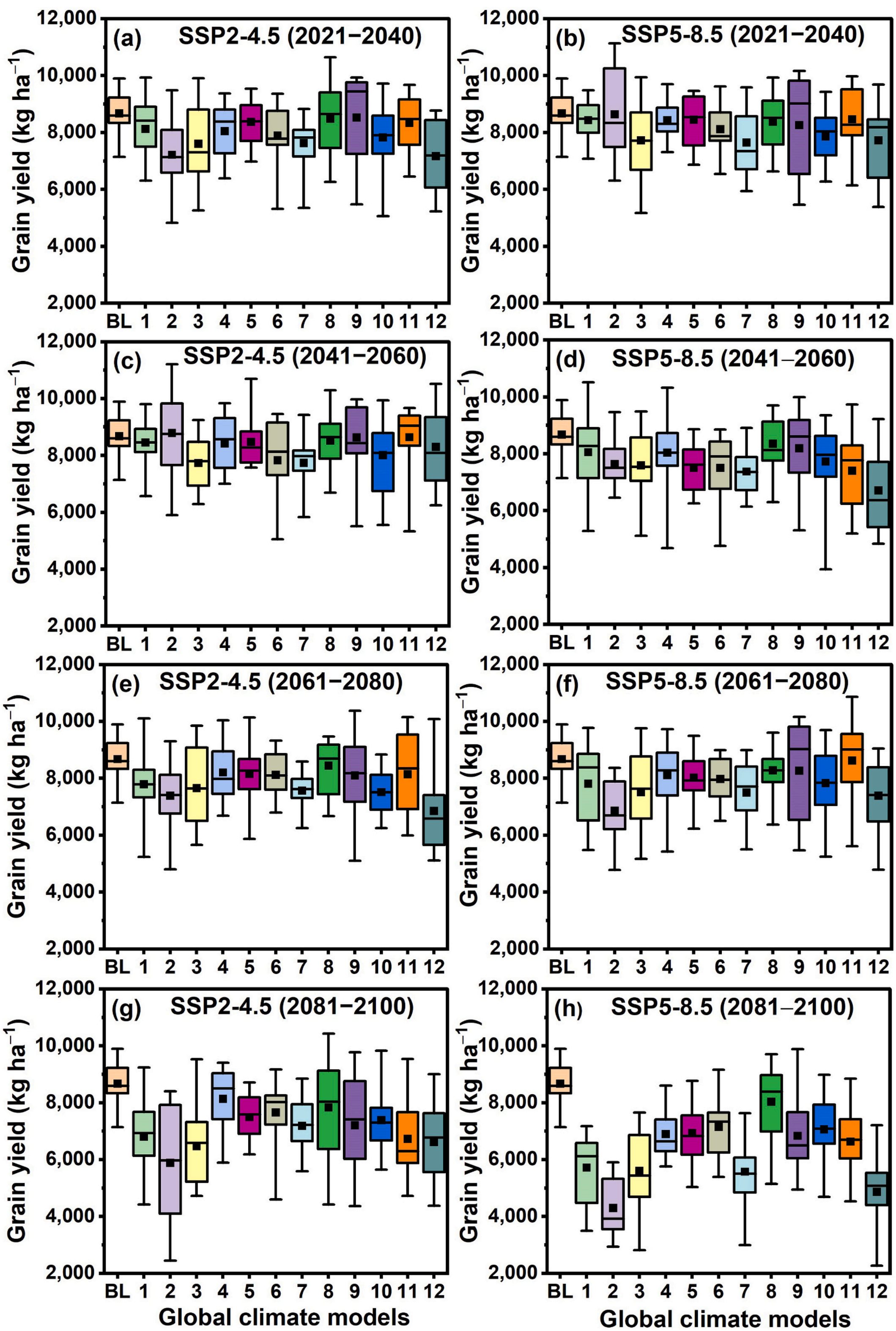

Fig. 5. The CROPSIM CERES-Wheat model projected the warming climate and precipitation impact on winter wheat grain yield in Terms 1, 2, 3, and 4 under SSP2–4.5 (a,c,e, and g) and SSP5–8.5 (b,d,f, and h) scenarios. Where BL represents the baseline, and 1 (ACCESS-CM2), 2 (CanESM5), 3 (EC-Earth3), 4 (GFDL-CM4), 5 (GFDL-ESM4), 6 (INM-CM5–0), 7 (IPSL-CM6A-LR), 8 (MIROC6), 9 (MPI-ESM1.2-LR), 10 (MRI-ESM2–0), 11 (NorESM2-LM), and 12 (TaiESM1) represent GCMs.

winter wheat in response to changing climatic conditions and investigated the impact of different levels of N fertilizer treatments, ranging from 0 to 400 kg ha^{-1}, on grain yield (Fig. 11). The results of our study showed a gradual rise in crop yields as the amount of N fertilizer used increased. The highest average grain yields were 8452 kg ha^{-1} (CROPSIM CERES-Wheat) and 8489 kg ha^{-1} (NWheat) when 400 kg ha^{-1} was applied. Nevertheless, even at lower application rates, the yields were significant. Specifically, at a rate of 350 kg ha^{-1}, the yields were 8209 kg ha^{-1} (CROPSIM CERES-Wheat) and 8246 kg ha^{-1} (NWheat). Similarly, at a farmer practice rate of 300 kg ha^{-1}, the yields

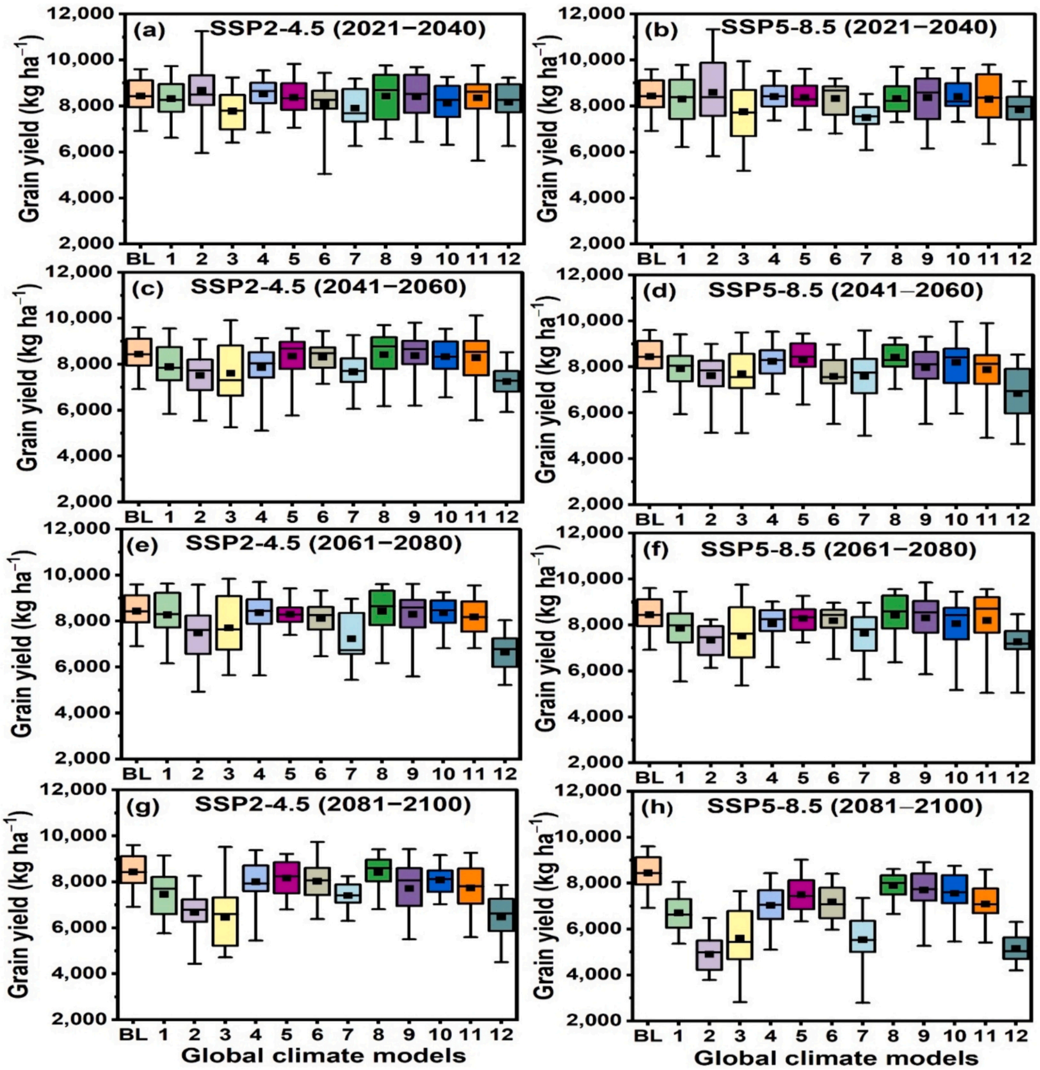

Fig. 6. DSSAT NWheat model projected warming climate and precipitation impact on winter wheat grain yield in Term 1, 2, 3, and 4 under SSP2–4.5 (a,c,e, and g) and SSP5–8.5 (b,d,f, and h) scenarios. Where BL represents the baseline, and 1 (ACCESS-CM2), 2 (CanESM5), 3 (EC-Earth3), 4 (GFDL-CM4), 5 (GFDL-ESM4), 6 (INM-CM5–0), 7 (IPSL-CM6A-LR), 8 (MIROC6), 9 (MPI-ESM1.2-LR), 10 (MRI-ESM2–0), 11 (NorESM2-LM), and 12 (TaiESM1) represent GCMs.

were 7852 kg ha^{-1} (CROPSIM CERES-Wheat) and 7893 kg ha^{-1} (NWheat). Conversely, reducing the N application to 250 kg ha^{-1} led to only a minor 5% decrease in yields compared to the farming practice. Conversely, the lack of N fertilizer led to a substantial decrease in crop production, resulting in minimum average grain yields of 1808–1813 kg ha^{-1}.

A comprehensive assessment of improvements in yield across the range of N application levels revealed that the yield gain between 250 kg ha^{-1} and 400 kg ha^{-1} was not significantly substantial. Based on this finding, it is concluded that applying optimal N at a rate of 250–300 kg ha^{-1} would be the most effective in achieving maximum grain yields for winter wheat under warming conditions.

3.7.4. *Adaptive irrigation practices for maximizing grain yield under warming climate*

This study conducted a thorough analysis of the effects of different irrigation applications, ranging from 0 to 500 mm, on grain yield using the DSSAT CROPSIM-CERES Wheat and NWheat models (Fig. 12). The mean grain yields peaked at 8031 kg ha^{-1} (CROPSIM CERES-Wheat) and 8211 kg ha^{-1} (NWheat) at 400 mm irrigation level, surpassing the yields observed at different irrigation rates. The yields were marginally reduced to 500 mm, measuring 7915 kg ha^{-1} (CROPSIM CERES-Wheat) and 8100 kg ha^{-1} (NWheat). The yields obtained from conventional irrigation at 300 mm were 7853 kg ha^{-1} (CROPSIM CERES-Wheat) and 7932 kg ha^{-1} (NWheat). However, the irrigation level of 200 mm showed an 18 to 22% decrease in average grain as evaluated by the CROPSIM CERES-Wheat and NWheat models compared to conventional practice irrigation. In the absence of irrigation, crop yield experienced a substantial decline to a range of 1482–1843 kg ha^{-1}. Compared with the traditional practice of 300 mm, a slight increase in production of 1–4% was observed when using irrigation levels of 400–500 mm. Based on our findings, we recommend an irrigation range of 300–400 mm as the optimal strategy for maximizing winter wheat yields under projected warmer conditions.

4. Discussion

4.1. *Crop simulation models and calibration*

Climate change impacts are better estimated using multi-model climate forecasts than using a single model (Asseng et al., 2015; Ali et al., 2020). Therefore, in this study, we incorporated NWheat with CROPSIM CERES-Wheat, a novel derivative model that has recently been incorporated into previous DSSAT models (Kassie et al., 2016). A

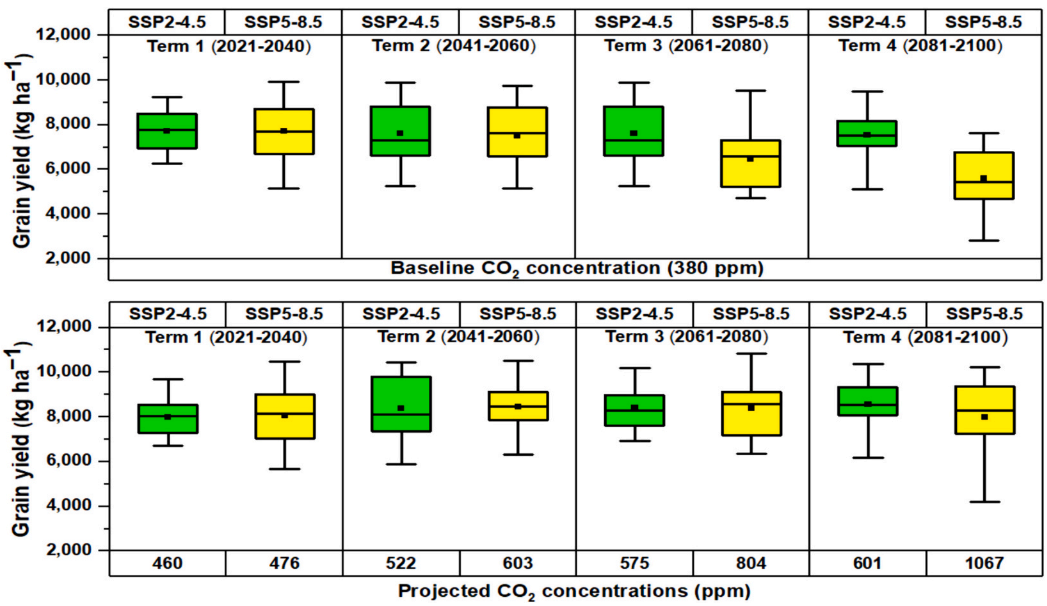

Fig. 7. Impact of baseline and projected CO_2 concentrations on CROPSIM CERES-Wheat predicted winter wheat grain yield in warming climate in Terms 1,2,3, and 4 under SSP2–4.5 and SSP5–8.5 scenarios.

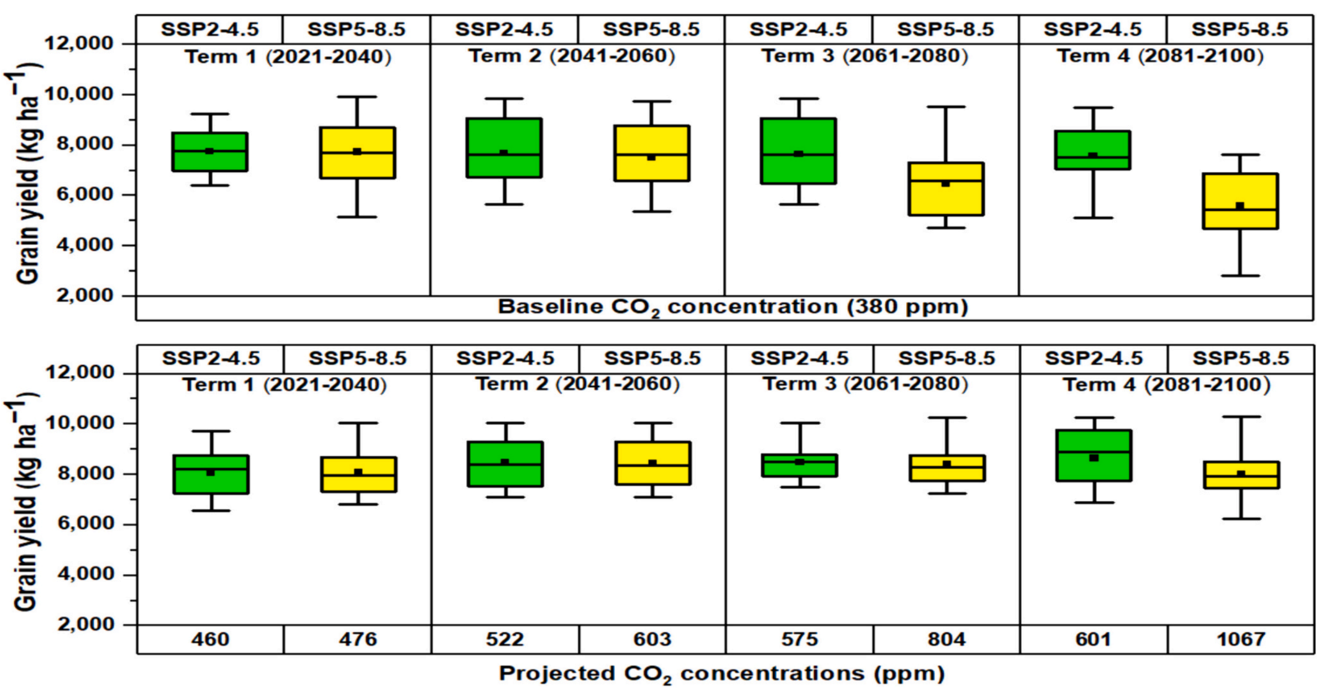

Fig. 8. The impact of baseline and projected CO_2 concentrations on NWheat predicted winter wheat grain yield in the warming climate in Terms 1,2,3, and 4 under the SSP2–4.5, and SSP5–8.5 scenarios.

good fit was demonstrated between the observed and simulated values of phenology, grain number, and grain yield for both models (Ali et al., 2020; Timsina et al., 2008). The models demonstrated good performance as measured by RMSE, nRMSE, and d, which aligns well with the existing literature (Ahmed et al., 2016; Timsina et al., 2008).

4.2. Climate change projections and impacts on winter wheat production

GCMs of CMIP6 showed the increase in maximum temperature, minimum temperature and variability in precipitation from Term 1 to Term 4 under SSP2–4.5 and SSP5–8.5 scenarios. The projections from the SSP2–4.5 to SSP5–8.5 scenarios showed a wide but more concerning range of outcomes. In the SSP5–8.5 scenario, temperature rises are more significant due to higher emissions (Liu et al., 2021b) and concentrations, resulting in greater radiative forcing (O'Neill et al., 2017). From Term 1 to the end Term 4, these changes are not static, but gradually intensify, correlating with other studies (Wen et al., 2023; Tan et al., 2023; Ishaque et al., 2023). CMIP6 GCMs projected a significant increase in precipitation by the end of the century (Du et al., 2022). Tian and Dong (2020) observed that addressing the double-ITCZ bias and associated precipitation bias in CMIP6 models, with the incorporation of the Cloud Feedback Model Intercomparison Project (CFMIP), highlights

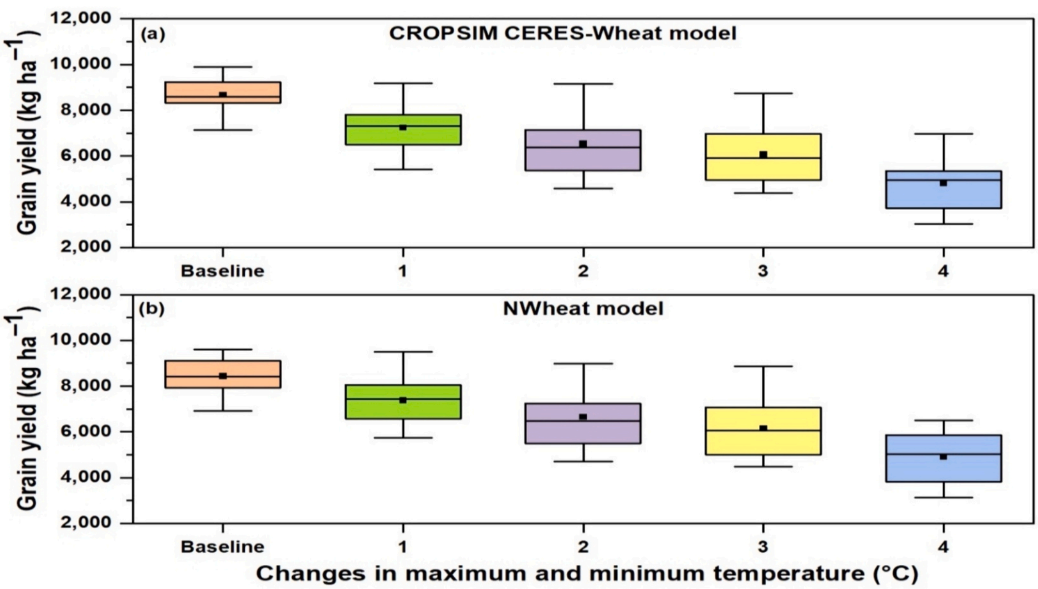

Fig. 9. CROPSIM CERES-Wheat (a) and NWheat (b) model sensitivity to temperature changes and projected winter wheat grain yield under baseline climate data.

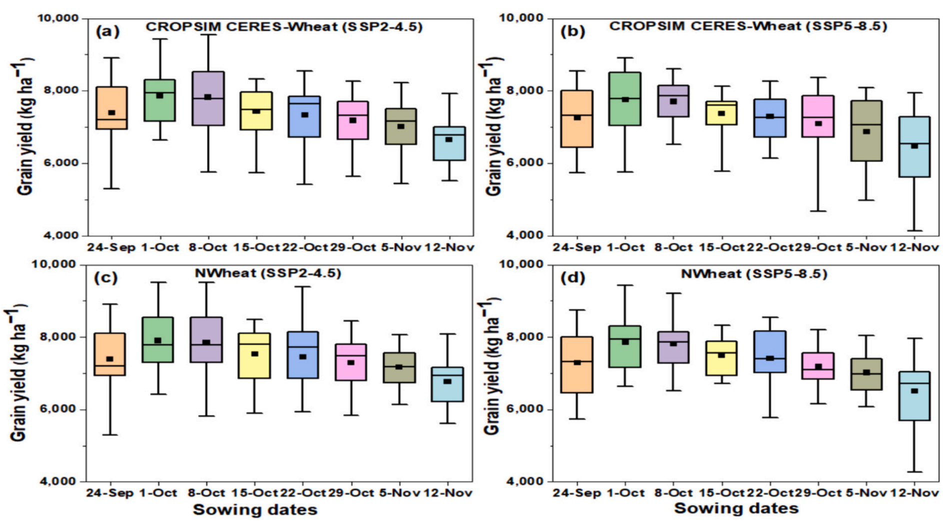

Fig. 10. CROPSIM CERES-Wheat (a) and (b) and NWheat (c) and (d) models projected the impact of sowing dates on winter wheat grain yield in a warming climate in term 1 under the SSP2–4.5 (a and c) and SSP5–8.5 (b and d) scenarios.

significant advancements over CMIP5, likely contributing to the increased precipitation projections (Eyring et al., 2016). Incremental warming and variable precipitation primarily lead to shortened growth periods and decreased grain number and yield, which can adversely impact food security. The effects were notably more severe under SSP5–8.5 scenario, because of higher temperature increases and greater precipitation variability (Eyring et al., 2016), intensifying thermal stress and disrupting the phenological development of wheat, which results in reduced yield (Asseng et al., 2015). This progression from Term 1 to Term 4 underscores the escalating nature of climatic stressors, with the most substantial impacts observed by the end of century Term 4 (Ishaque et al., 2023; Liu et al., 2021b). This pattern is in line with global climate projections that predict the intensification of climatic extremes towards the end of the century (IPCC, 2021; IPCC, 2022; IPCC, 2023). Further corroborated by other studies, these dynamics illustrate that rising temperatures accelerate growth and developmental phases, shortening the life cycle (Liu et al., 2021b; Muleke et al., 2022), impairing canopy development, reducing photosynthetic activity, and increasing respiration rates (Ali et al., 2020; Li and Lei, 2022). This rising temperature leads to faster development and a shorter period of grain filling, which is essential for yield accumulation (Shoukat et al., 2022). Wen et al. (2023) observed that slight increases in precipitation cannot counterbalance the negative impacts of high temperatures. Notably, Lopes (2022) found that, in northeastern European countries, wheat yields do not necessarily benefit from a rise in temperature or precipitation. Our findings resonate with other regional studies, indicating a consistent trend of climatic stress exacerbation over time, necessitating advanced adaptive strategies to safeguard winter wheat production against future climatic adversities (Yang et al., 2019).

This underscores the urgency for targeted agricultural adaptations to address the anticipated challenges posed by climatic shifts in North China Plain, emphasizing the profound impact of model selection and setup on the accuracy of projecting climate change effects on winter wheat yields. We noticed that CERES-Wheat consistently displayed greater sensitivity to climate variability than NWheat among all GCMs, as confirmed by Kassie et al. (2016). These findings indicate that the way the chosen crop model is designed and set up can greatly influence the accuracy of predicting the impact of climatic conditions, such as

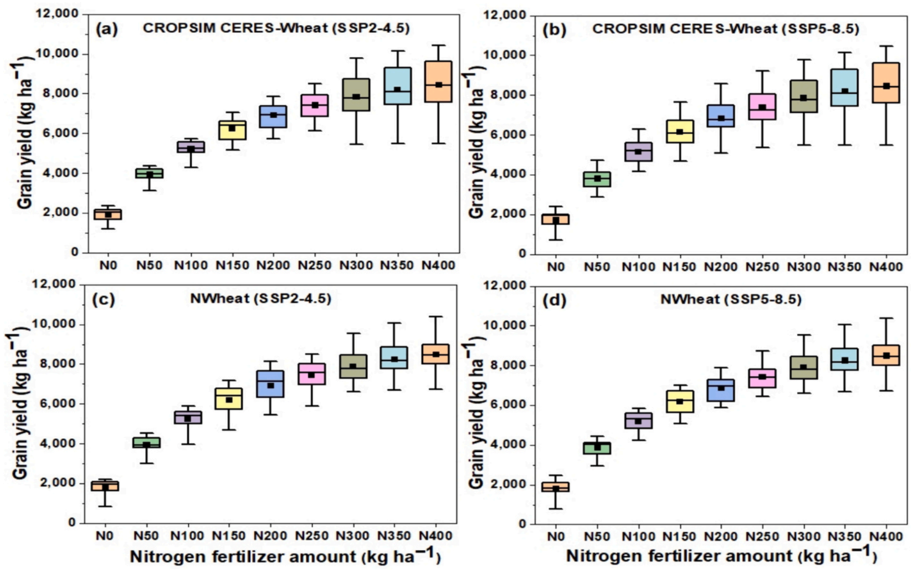

Fig. 11. CROPSIM CERES-Wheat (a) and (b) and NWheat (c) and (d) models projected the impact of N fertilizer rates on winter wheat grain yield in a warming climate in term 1 under the SSP2–4.5 (a and c) and SSP5–8.5 (b and d) scenarios.

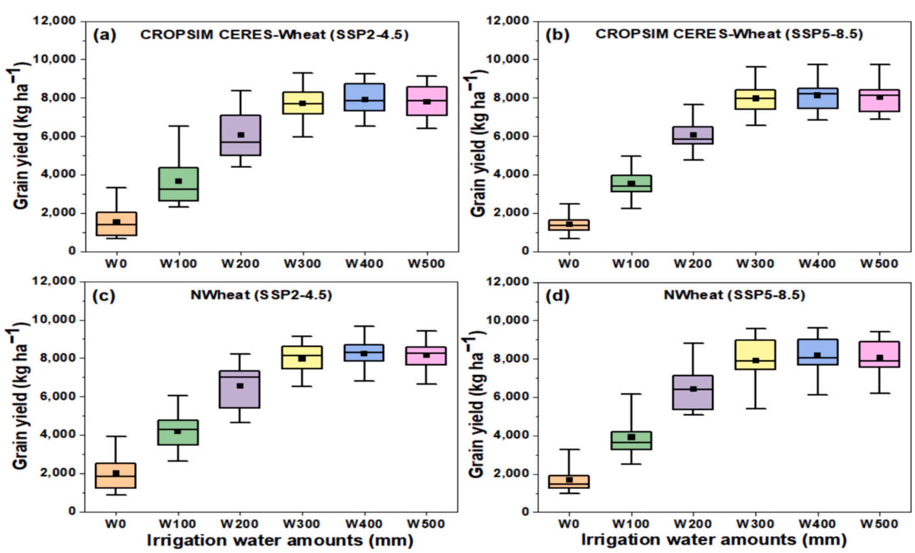

Fig. 12. CROPSIM CERES-Wheat (a) and (b) and NWheat (c) and (d) models projected the impact of irrigation water amounts on winter wheat grain yield in a warming climate in term 1 under the SSP2–4.5 (a and c) and SSP5–8.5 (b and d) scenarios.

temperature and increased CO_2 levels, on winter wheat yields.

4.3. Impact of future CO_2 concentrations on grain yield

This study demonstrated a direct correlation between increasing CO_2 levels and the yield of winter wheat grains, aligning with prior studies conducted on C3 grass species (Asseng et al., 2019). Specifically, under the SSP5–8.5 scenario for Term 4, our projections with the CROPSIM CERES-Wheat and NWheat models anticipated a significant 30% increase in crop yield, attributed to higher CO_2 concentrations (Tan et al., 2023). The increased production of grains is due to the improved absorption of carbon during photosynthesis, more efficient utilization of nitrogen, and less water loss caused by partially closed stomata under higher CO_2 environments (Asseng et al., 2019; Tan et al., 2023). Interestingly, Term 1 displayed negligible yield differences across scenarios due to lower CO_2 concentrations, but a clear trend of increasing benefits was observed in later terms (Term 2 to 4). This progression suggests that a long-term rise in CO_2 levels could potentially mitigate some of the negative impacts of climate change on winter wheat production in the region (Tan et al., 2023; Asseng et al., 2019).

4.4. Sensitivity analysis to temperature changes and adaptive strategies in warming climate

According to the NWheat and CROPSIM CERES-Wheat models, winter wheat production is highly sensitive to changes in temperature. Both models demonstrated that rising temperatures led to a decrease in yield. This increase in temperature results in accelerated development and a reduced duration of grain filling, which is crucial for yield accumulation (Shoukat et al., 2022). This study emphasizes the necessity of integrated management strategies to bolster crop resilience amidst global warming. This study investigated various adaptation measures tailored to minimize the effects of climate change on winter wheat grain yield in the NCP. Strategies such as optimizing planting dates, managing nitrogen fertilizer use, and adjusting irrigation levels are proactive steps to sustain and improve agricultural productivity under variable climatic conditions. Similarly, Muleke et al. (2023) developed adaptation strategies focusing on irrigation, fertilizer application, and sowing dates to enhance soil organic carbon dynamics and agricultural sustainability.

In regions like the North China Plain, where winters are warming, adjusting sowing dates for winter wheat is crucial. Timely sowing is a key adaptation strategy to ensure optimal growth in warmer climates (Jiang et al., 2023). Our study emphasizes the importance of planting during the optimal window the first week of October to maximize yield and crop health in a changing climate. Early sowing in October can promote faster growth during the initial stages and help maintain proper coverage of winter wheat during the dormancy period, which is crucial for overall crop health and productivity (Liu et al., 2021a). Sowing seeds before October can lead to early growth that does not align with ideal conditions, increasing seedling vulnerability to temperature stress, pests, and diseases, which may limit yield potential (Peake et al., 2016).). Conversely, delaying sowing past the first week of October can misalign with favorable conditions, raising risks of frost damage, disrupted flowering, and increased susceptibility to heat stress, pests, and diseases all factors that reduce crop output (Fang et al., 2013; Wang et al., 2012; Zhou et al., 2020). These studies indicate that deviations from the optimal sowing period can result in significant yield losses in a changing climate.

Our study found that winter wheat grain yield increased with N fertilizer applications up to 400 kg ha^{-1}. However, the most substantial yield improvements occurred between 250 and 300 kg ha^{-1}, with no significant increase beyond this range. This aligns with optimal N management principles for sustainability(Tilman et al., 2002). The lack of yield increase above 300 kg ha^{-1} is likely due to the crop reaching its physiological nitrogen use efficiency limit (Mueller et al., 2012). Excessive N application poses environmental risks, such as nitrate leaching and greenhouse gas emissions, highlighting the need for balanced fertilization (Erisman et al., 2008). Therefore, we recommend an N application rate of 250–300 kg ha^{-1} to optimize grain yield while minimizing environmental harm under warming conditions (Huang et al., 2015). In the agriculturally intensive NCP, our findings align with local studies, emphasizing the necessity of optimized N management to sustain yields and reduce environmental impacts (Chen et al., 2011; Huang et al., 2015). These results support a balanced N fertilization approach as an adaptation strategy for improving crop yield and environmental sustainability in the context of climate change.

Our study demonstrated that adjusting irrigation levels for winter wheat in a warming climate positively affects grain yield, aligning with Gao et al. (2024) who found that irrigation application can enhance winter wheat yields even under severe climate change scenarios. Our study found that maintaining irrigation within the optimal range of 300–400 mm is beneficial, as it balances soil moisture availability with the physiological needs of the crop, thereby optimizing photosynthesis and nutrient uptake during key growth phases (Touil et al., 2022). Inadequate irrigation fails to satisfy the heightened water demands of wheat in warmer conditions, inducing stress that can significantly reduce grain yield (Tack et al., 2017). On the other hand, over-irrigation, such as applying 500 mm, offers no additional benefits and can lead to adverse effects like soil compaction, reduced aeration, nutrient leaching, and an increase in root diseases (Qureshi, 2014). Adhering to the optimal irrigation range not only maximizes wheat yield but also conserves water resources, addressing both water scarcity and climate change challenges. This strategic approach ensures that agricultural practices meet plant physiological needs and environmental conservation, making it a crucial component of adaptive strategies for sustainable water use and enhanced resilience in agriculture.

4.5. Study limitations and future research directions

This study utilized the GCMs of CMIP6, which offers a more reliable basis for future climate projections compared to earlier versions (Eyring et al., 2016). However, this study acknowledges the limitations of relying solely on climate and cropping-system models. The use of 12 GCMs from >55 available models may limit the generalizability of our findings. Additionally, this study focused on a single climate zone in which the study area was located. For future research, incorporating a wider array of CMIP6 GCMs and crop system models is recommended to enhance the robustness of the climate projections. It is also important to investigate the impact of global warming on specific yield parameters, such as leaf area index, 1000-grain weight, and total dry matter. Exploring the differences between crop models (e.g., AgMIP) and GCMs can provide deeper insights into the uncertainties and potential impacts of climate change on agriculture. Developing tailored adaptation strategies for the various climatic zones of the NCP agro-ecosystems will help mitigate the adverse effects on winter wheat production.

5. Conclusion

In this research, we demonstrated using DSSAT CROPSIM CERES-Wheat and NWheat models that climatic warming and changes in precipitation significantly impact the phenology, grain numbers, and yields of winter wheat. Our simulations, based on CMIP6 GCMs and different climate scenarios for the 21st century, indicate that temperature is likely to increase by 0.82–3.13 °C and seasonal precipitation could rise by 13–36% under the SSP2–4.5 and SSP5–8.5 scenarios compared to baseline data. These changes are projected to shorten the winter wheat growing season by 4–17% and decrease grain number and yield by 3–21%. However, moderate increases in average maximum (0.89 °C) and minimum (0.74 °C) temperatures, along with an 8% rise in seasonal precipitation under the same scenarios, are expected to enhance grain yields by 0.16–2.90% for the period 2021–2040. Furthermore, rising CO_2 concentrations could potentially increase grain yields by 4–30% from 2021 to 2100 under the SSP5–8.5 scenario, thereby mitigating some of the negative effects of climate warming. These findings highlight the need to incorporate heat sensitivity into crop models and develop resilient agricultural practices. Key strategies, such as planting winter wheat in the first week of October and providing optimal irrigation (300–400 mm) and nitrogen levels (250–300 kg ha^{-1}), can mitigate the adverse effects of warming. These methods offer actionable guidance for policymakers, farmers, and researchers to develop sustainable agricultural practices and ensure food security in the changing climate. Future research should extend these insights to additional crops and examine the enduring impacts of climate change on crop yields in various climatic zones using advanced models. This broader scope is crucial for crafting comprehensive strategies to sustain global food production amidst climates.

CRediT authorship contribution statement

Muhammad Rizwan Shoukat: Writing – original draft, Software, Methodology, Investigation, Formal analysis, Data curation, Conceptualization. **Jingjing Wang:** Writing – review & editing, Visualization, Validation, Data curation. **Muhammad Habib-ur-Rahman:** Writing – review & editing, Validation, Software, Methodology, Data curation, Conceptualization. **Xin Hui:** Writing – review & editing, Visualization, Validation, Data curation. **Gerrit Hoogenboom:** Writing – review & editing, Validation, Software, Methodology. **Haijun Yan:** Writing – review & editing, Validation, Supervision, Software, Resources, Project administration, Methodology, Funding acquisition, Formal analysis, Conceptualization.

Declaration of competing interest

The authors declare that they have no known competing financial interests or personal relationships that could have appeared to influence the work reported in this paper.

Data availability

Data will be made available on request.

Acknowledgements

This work was supported by grants from the Key Research and Development Program of Hebei Province (Grant No. 21327002D), Water Conservancy Technology Demonstration Project of Ministry of Water Resources of China (Grant No. SF-202311) and China Agriculture Research System (Grant No. CARS-03).

Appendix A. Supplementary data

Supplementary data to this article can be found online at https://doi.org/10.1016/j.agsy.2024.104066.

References

Ahmad, I., Ahmad, B., Boote, K., Hoogenboom, G., 2020. Adaptation strategies for maize production under climate change for semi-arid environments. Eur. J. Agron. 115, 126040.

Ahmed, M., Akram, M.N., Asim, M., Aslam, M., Hassan, F.-U., Higgins, S., Stöckle, C.O., Hoogenboom, G., 2016. Calibration and validation of APSIM-wheat and CERES-wheat for spring wheat under rainfed conditions: models evaluation and application. Comput. Electron. Agric. 123, 384–401. https://doi.org/10.1016/j.compag.2016.03.015.

Ali, M.G.M., Ibrahim, M.M., El Baroudy, A., Fullen, M., Omar, E.-S.H., Ding, Z., Kheir, A.M.S., 2020. Climate change impact and adaptation on wheat yield, water use and water use efficiency at North Nile Delta. Front. Earth Sci. 14, 522–536. https://doi.org/10.1007/s11707-019-0806-4.

Ashfaq, M., Rastogi, D., Kitson, J., Abid, M.A., Kao, S.C., 2022. Evaluation of CMIP6 GCMs over the CONUS for downscaling studies. J. Geophys. Res. Atmos. 127 https://doi.org/10.1029/2022JD036659 e2022JD036659.

Asseng, S., Jamieson, P., Kimball, B., Pinter, P., Sayre, K., Bowden, J., Howden, S., 2004. Simulated wheat growth affected by rising temperature, increased water deficit and elevated atmospheric CO2. Field Crop Res 85, 85–102. https://doi.org/10.1016/S0378-4290(03)00154-0.

Asseng, S., Ewert, F., Martre, P., Rötter, R.P., Lobell, D.B., Cammarano, D., Kimball, B.A., Ottman, M.J., Wall, G.W., White, J.W., 2015. Rising temperatures reduce global wheat production. Nature climate change 5, 143–147.

Asseng, S., Martre, P., Maiorano, A., Rötter, R.P., O'Leary, G.J., Fitzgerald, G.J., Girousse, C., Motzo, R., Giunta, F., Babar, M.A., 2019. Climate change impact and adaptation for wheat protein. Glob. Chang. Biol. 25, 155–173. https://doi.org/10.1111/gcb.14481.

Chen, X.-P., Cui, Z.-L., Vitousek, P.M., Cassman, K.G., Matson, P.A., Bai, J.-S., Meng, Q.-F., Hou, P., Yue, S.-C., Römheld, V., 2011. Integrated soil–crop system management for food security. Proc. Natl. Acad. Sci. 108, 6399–6404.

Du, Y., Wang, D., Zhu, J., Wang, D., Qi, X., Cai, J., 2022. Comprehensive assessment of CMIP5 and CMIP6 models in simulating and projecting precipitation over the global land. Int. J. Climatol. 42, 6859–6875. https://doi.org/10.1002/joc.7616.

Erisman, J.W., Sutton, M.A., Galloway, J., Klimont, Z., Winiwarter, W., 2008. How a century of ammonia synthesis changed the world. Nat. Geosci. 1, 636–639. https://doi.org/10.1038/ngeo325.

Eyring, V., Bony, S., Meehl, G.A., Senior, C.A., Stevens, B., Stouffer, R.J., Taylor, K.E., 2016. Overview of the coupled model Intercomparison project phase 6 (CMIP6) experimental design and organization. Geosci. Model Dev. 9, 1937–1958. https://doi.org/10.5194/gmd-9-1937-2016.

Fang, Q., Ma, L., Green, T., Yu, Q., Wang, T., Ahuja, L., 2010. Water resources and water use efficiency in the North China plain: current status and agronomic management options. Agric Water Manag 97, 1102–1116. https://doi.org/10.1016/j.agwat.2010.01.008.

Fang, S., Su, H., Liu, W., Tan, K., Ren, S., 2013. Infrared warming reduced winter wheat yields and some physiological parameters, which were mitigated by irrigation and worsened by delayed sowing. PloS One 8, e67518.

Gao, Y., Wang, L., Yue, Y., 2024. Impact of irrigation on vulnerability of winter wheat under extreme climate change scenario: a case study of North China Plain. Frontiers in Sustainable Food Systems 7, 1291866. https://doi.org/10.3389/fsufs.2023.1291866.

Gul, F., Ahmed, I., Ashfaq, M., Jan, D., Fahad, S., Li, X., Wang, D., Fahad, M., Fayyaz, M., Shah, S.A., 2020. Use of crop growth model to simulate the impact of climate change on yield of various wheat cultivars under different agro-environmental conditions in Khyber Pakhtunkhwa, Pakistan. Arab. J. Geosci. 13, 1–14. https://doi.org/10.1007/s12517-020-5118-1.

Han, W., Lin, X., Wang, D., 2023. Uncovering the primary drivers of regional variability in the impact of climate change on wheat yields in China. J. Clean. Prod. 138479 https://doi.org/10.1016/j.jclepro.2023.138479.

Hoogenboom, G., Porter, C.H., Boote, K.J., Shelia, V., Wilkens, P.W., Singh, U., White, J.W., Asseng, S., Lizaso, J.I., Moreno, L.P., Pawan, W., Ogoshi, R., Hunt, L.A., 2019. The DSSAT Crop Modeling Ecosystem. Burleigh Dodds Science Publishing, Cambridge, United Kingdom. https://doi.org/10.19103/AS.2019.0061.10.

Hoogenboom, G., Porter, C.H., Shelia, V., Boote, K.J., Singh, U., Pavan, W., Oliveira, F.A.A., Moreno-Cadena, L.P., Ferreira, T.B., White, J.W., Lizaso, J.I., Pequeno, D.N.L., Kimball, B.A., Alderman, P.D., Thorp, K.R., Cuadra, S.V., Vianna, M.S., Villalobos, F.J., Batchelor, W.D., Asseng, S., Jones, M.R., Hopf, A., Dias, H.B., Hunt, L.A., Jones, J.W., 2023. Decision Support System for Agrotechnology Transfer (DSSAT) version 4.8.0 (www.DSSAT.net). DSSAT Foundation, Gainesville, Florida, USA.

Huang, J., Huang, Z., Jia, X., Hu, R., Xiang, C., 2015. Long-term reduction of nitrogen fertilizer use through knowledge training in rice production in China. Agr. Syst. 135, 105–111. https://doi.org/10.1016/j.agsy.2015.01.004.

Hui, X., Lin, X., Zhao, Y., Xue, M., Zhuo, Y., Guo, H., Xu, Y., Yan, H., 2022. Assessing water distribution characteristics of a variable-rate irrigation system. Agric Water Manag 260, 107276. https://doi.org/10.1016/j.agwat.2021.107276.

IPCC, 2021. Intergovernmental panel on climate, change 2021 – The physical science basis: Working group I contribution to the sixth assessment report of the intergovernmental panel on climate change. In: Cambridge University Press, Cambridge, UK and New York, USA. Cambridge University Press, Cambridge, UK and New York, USA.

IPCC, 2022. Intergovernmental Panel on Climate, Change 2022 – Impacts, Adaptation and Vulnerability: Working Group II Contribution to the Sixth Assessment Report of the Intergovernmental Panel on Climate Change. Cambridge University Press, Cambridge, UK and New York, USA.

IPCC, 2023. Summary for policymakers. In: Climate Change 2023: Synthesis Report.A Report of the Intergovernmental Panel on Climate Change. Contribution of Working Groups I, II and III to the Sixth Assessment Report of the Intergovernmental Panel on Climate Change [Core Writing Team, H. Lee and J. Romero (eds.)]. IPCC, Geneva, Switzerland.

Iqbal, Z., Shahid, S., Ahmed, K., Ismail, T., Ziarh, G.F., Chung, E.-S., Wang, X., 2021. Evaluation of CMIP6 GCM rainfall in mainland Southeast Asia. Atmos. Res. 254, 105525 https://doi.org/10.1016/j.atmosres.2021.105525.

Ishaque, W., Osman, R., Hafiza, B.S., Malghani, S., Zhao, B., Xu, M., Ata-Ul-Karim, S.T., 2023. Quantifying the impacts of climate change on wheat phenology, yield, and evapotranspiration under irrigated and rainfed conditions. Agric Water Manag 275, 108017. https://doi.org/10.1016/j.agwat.2022.108017.

Jia, X., Shao, L., Liu, P., Zhao, B., Gu, L., Dong, S., Bing, S.H., Zhang, J., Zhao, B., 2014. Effect of different nitrogen and irrigation treatments on yield and nitrate leaching of summer maize (Zea mays L.) under lysimeter conditions. Agric Water Manag 137, 92–103. https://doi.org/10.1016/j.agwat.2014.02.010.

Jiang, T., Wang, B., Duan, X., Li Liu, D., He, J., He, L., Jin, N., Feng, H., Yu, Q., 2023. Prioritizing agronomic practices and uncertainty assessment under climate change for winter wheat in the loess plateau, China. Agricultural Systems 212, 103770. https://doi.org/10.1016/j.agsy.2023.103770.

Jones, J.W., Hoogenboom, G., Porter, C.H., Boote, K.J., Batchelor, W.D., Hunt, L., Wilkens, P.W., Singh, U., Gijsman, A.J., Ritchie, J.T., 2003. The DSSAT cropping system model. Eur. J. Agron. 18, 235–265. https://doi.org/10.1016/S1161-0301(02)00107-7.

Kassie, B.T., Asseng, S., Porter, C.H., Royce, F.S., 2016. Performance of DSSAT-Nwheat across a wide range of current and future growing conditions. Eur. J. Agron. 81, 27–36. https://doi.org/10.1016/j.eja.2016.08.012.

Kheir, A.M., El Baroudy, A., Aiad, M.A., Zoghdan, M.G., Abd El-Aziz, M.A., Ali, M.G., Fullen, M.A., 2019. Impacts of rising temperature, carbon dioxide concentration and sea level on wheat production in North Nile delta. Sci. Total Environ. 651, 3161–3173. https://doi.org/10.1016/j.scitotenv.2018.10.209.

Kong, X., Hou, R., Yang, G., Ouyang, Z., 2023. Climate warming extends the effective growth period of winter wheat and increases grain protein content. Agric. For. Meteorol. 336, 109477 https://doi.org/10.1016/j.agrformet.2023.109477.

Li, J., Lei, H., 2022. Impacts of climate change on winter wheat and summer maize dual-cropping system in the North China plain. Environmental Research Communications 4, 075014. https://doi.org/10.1088/2515-7620/ac814c.

Li, S., Lu, Z., Zhao, J., Luo, M., Chen, F., Chu, Q., 2023. Changes in planting methods will change the potential distribution of rice in South China under climate warming. Agric. For. Meteorol. 331, 109355 https://doi.org/10.1016/j.agrformet.2023.109355.

Li, N., Li, Y., Yang, Q., Biswas, A., Dong, H., 2024. Simulating climate change impacts on cotton using AquaCrop model in China. Agr. Syst. 216, 103897 https://doi.org/10.1016/j.agsy.2024.103897.

Liang, Z., Sun, L., Tian, Z., Fischer, G., Yan, H., 2023. Increase in grain production potential of China under climate change. PNAS Nexus 2, pgad057. https://doi.org/10.1093/pnasnexus/pgad057.

Liu, F., Chen, Y., Bai, N., Xiao, D., Bai, H., Tao, F., Ge, Q., 2021a. Divergent climate feedbacks on winter wheat growing and dormancy periods as affected by sowing date in the North China plain. Biogeosciences 18, 2275–2287. https://doi.org/10.5194/bg-18-2275-2021.

Liu, K., Harrison, M.T., Archontoulis, S.V., Huth, N., Yang, R., Liu, D.L., Yan, H., Meinke, H., Huber, I., Feng, P., 2021b. Climate change shifts forward flowering and reduces crop waterlogging stress. Environ. Res. Lett. 16, 094017 https://doi.org/10.1088/1748-9326/ac1b5a.

Lobell, D.B., Tebaldi, C., 2014. Getting caught with our plants down: the risks of a global crop yield slowdown from climate trends in the next two decades. Environ. Res. Lett. 9, 074003 https://doi.org/10.1088/1748-9326/9/7/074003.

Lopes, M.S., 2022. Will temperature and rainfall changes prevent yield progress in Europe? Food and Energy Security 11, e372. https://doi.org/10.1002/fes3.372.

Mueller, N.D., Gerber, J.S., Johnston, M., Ray, D.K., Ramankutty, N., Foley, J.A., 2012. Closing yield gaps through nutrient and water management. Nature 490, 254–257. https://doi.org/10.1038/nature11420.

Muleke, A., Harrison, M.T., De Voil, P., Hunt, I., Liu, K., Yanotti, M., Eisner, R., 2022. Earlier crop flowering caused by global warming alleviated by irrigation. Environ. Res. Lett. 17, 044032 https://doi.org/10.1088/1748-9326/ac5a66.

Muleke, A., Harrison, M.T., Eisner, R., Yanotti, M., de Voil, P., Fahad, S., Fei, W., Feng, P., Ferreira, C., Forster, D., 2023. Clarifying confusions over carbon conclusions: antecedent soil carbon drives gains realised following intervention. Global Environmental Change Advances 1, 100001. https://doi.org/10.1016/j.gecadv.2023.100001.

O'Neill, B.C., Kriegler, E., Ebi, K.L., Kemp-Benedict, E., Riahi, K., Rothman, D.S., Van Ruijven, B.J., Van Vuuren, D.P., Birkmann, J., Kok, K., 2017. The roads ahead: narratives for shared socioeconomic pathways describing world futures in the 21st century. Glob. Environ. Chang. 42, 169–180. https://doi.org/10.1016/j.gloenvcha.2015.01.004.

O'Neill, B.C., Carter, T.R., Ebi, K., Harrison, P.A., Kemp-Benedict, E., Kok, K., Kriegler, E., Preston, B.L., Riahi, K., Sillmann, J., 2020. Achievements and needs for the climate change scenario framework. Nat. Clim. Chang. 10, 1074–1084. https://doi.org/10.1038/s41558-020-00952-0.

Osman, R., Zhu, Y., Ma, W., Zhang, D., Ding, Z., Liu, L., Tang, L., Liu, B., Cao, W., 2020. Comparison of wheat simulation models for impacts of extreme temperature stress on grain quality. Agric. For. Meteorol. 288, 107995 https://doi.org/10.1016/j.agrformet.2020.107995.

Peake, A., Bell, K., Carberry, P., Poole, N., Raine, S., 2016. Vegetative nitrogen stress decreases lodging risk and increases yield of irrigated spring wheat in the subtropics. Crop and Pasture Science 67, 907–920. https://doi.org/10.1071/CP16052.

Qureshi, A.S., 2014. Reducing carbon emissions through improved irrigation management: a case study from Pakistan. Irrig. Drain. 63, 132–138. https://doi.org/10.1002/ird.1795.

Riahi, K., Van Vuuren, D.P., Kriegler, E., Edmonds, J., O'neill, B.C., Fujimori, S., Bauer, N., Calvin, K., Dellink, R., Fricko, O., 2017. The shared socioeconomic pathways and their energy, land use, and greenhouse gas emissions implications: an overview. Glob. Environ. Chang. 42, 153–168. https://doi.org/10.1016/j.gloenvcha.2016.05.009.

Ritchie, J., 1985. Description and performance of CERES wheat: A user-oriented wheat yield model. In: ARS Wheat Yield Project, pp. 159–175.

Saddique, Q., Cai, H., Xu, J., Ajaz, A., He, J., Yu, Q., Wang, Y., Chen, H., Khan, M.I., Liu, D.L., 2020. Analyzing adaptation strategies for maize production under future climate change in Guanzhong plain, China. Mitig. Adapt. Strat. Glob. Chang. 25, 1523–1543. https://doi.org/10.1007/s11027-020-09935-0.

Salehnia, N., Hosseini, F., Farid, A., Kolsoumi, S., Zarrin, A., Hasheminia, M., 2019. Comparing the performance of dynamical and statistical downscaling on historical run precipitation data over a semi-arid region. Asia-Pac. J. Atmos. Sci. 55, 737–749. https://doi.org/10.1007/s13143-019-00112-1.

Shoukat, M.R., Cai, D., Shafeeque, M., Habib-ur-Rahman, M., Yan, H., 2022. Warming climate and elevated CO2 will enhance future winter wheat yields in North China region. Atmosphere 13, 1275. https://doi.org/10.3390/atmos13081275.

Si, Z., Zain, M., Li, S., Liu, J., Liang, Y., Gao, Y., Duan, A., 2021. Optimizing nitrogen application for drip-irrigated winter wheat using the DSSAT-CERES-wheat model. Agric Water Manag 244, 106592. https://doi.org/10.1016/j.agwat.2020.106592.

Tack, J., Barkley, A., Hendricks, N., 2017. Irrigation offsets wheat yield reductions from warming temperatures. Environ. Res. Lett. 12, 114027 https://doi.org/10.1088/1748-9326/aa8d27.

Tan, L., Zhang, X., Qi, J., Sun, D., Marek, G.W., Feng, P., Li, B., Li Liu, D., Li, B., Srinivasan, R., 2023. Assessment of the sustainability of groundwater utilization and crop production under optimized irrigation strategies in the North China plain under future climate change. Sci. Total Environ. 899, 165619 https://doi.org/10.1016/j.scitotenv.2023.165619.

Tebaldi, C., Debeire, K., Eyring, V., Fischer, E., Fyfe, J., Friedlingstein, P., Knutti, R., Lowe, J., O'Neill, B., Sanderson, B., 2020. Climate model projections from the scenario model intercomparison project (ScenarioMIP) of CMIP6. Earth System Dynamics Discussions 2020, 1–50. https://doi.org/10.5194/esd-12-253-2021.

Tian, B., Dong, X., 2020. The double-ITCZ bias in CMIP3, CMIP5, and CMIP6 models based on annual mean precipitation. Geophys. Res. Lett. 47 https://doi.org/10.1029/2020GL087232 e2020GL087232.

Tilman, D., Cassman, K.G., Matson, P.A., Naylor, R., Polasky, S., 2002. Agricultural sustainability and intensive production practices. Nature 418, 671–677. https://doi.org/10.1038/nature01014.

Timsina, J., Humphreys, E., 2006. Performance of CERES-Rice and CERES-Wheat models in rice–wheat systems: A review. Agr. Syst. 90, 5–31. https://doi.org/10.1016/j.agsy.2005.11.007.

Timsina, J., Godwin, D., Humphreys, E., Kukal, S., Smith, D., 2008. Evaluation of options for increasing yield and water productivity of wheat in Punjab, India using the DSSAT-CSM-CERES-Wheat model. Agric Water Manag 95, 1099–1110. https://doi.org/10.1016/j.agwat.2008.04.009.

Touil, S., Richa, A., Fizir, M., Argente Garcia, J.E., Skarmeta Gomez, A.F., 2022. A review on smart irrigation management strategies and their effect on water savings and crop yield. Irrig. Drain. 71, 1396–1416. https://doi.org/10.1002/ird.2735.

Ur Rahman, M.H., Ahmad, A., Wang, X., Wajid, A., Nasim, W., Hussain, M., Ahmad, B., Ahmad, I., Ali, Z., Ishaque, W., 2018. Multi-model projections of future climate and climate change impacts uncertainty assessment for cotton production in Pakistan. Agric. For. Meteorol. 253, 94–113. https://doi.org/10.1016/j.agrformet.2018.02.008.

Wang, J., Wang, E., Yang, X., Zhang, F., Yin, H., 2012. Increased yield potential of wheat-maize cropping system in the North China plain by climate change adaptation. Clim. Change 113, 825–840. https://doi.org/10.1007/s10584-011-0385-1.

Wang, D., Liang, Y., Liu, L., Huang, J., Yin, Z., 2023a. Crop production on the Chinese Loess Plateau under 1.5 and 2.0° C global warming scenarios. Sci. Total Environ. 166158 https://doi.org/10.1016/j.scitotenv.2023.166158.

Wang, Y., Liu, S., Shi, H., 2023b. Comparison of climate change impacts on the growth of C3 and C4 crops in China. Eco. Inform. 74, 101968 https://doi.org/10.1016/j.ecoinf.2022.101968.

Wang, L., Liu, X., Liu, X., Bao, X., Zhang, X., Yin, B., Wang, W., Wang, Y., Zhen, W., 2024a. Effects of spring limited irrigation on grain yield and root characteristics of winter wheat in groundwater-overexploitation areas in the North China plain. Agric Water Manag 294, 108729. https://doi.org/10.1016/j.agwat.2024.108729.

Wang, Y., Wang, Z., Wu, L., Li, H., Li, J., Zhu, A., Jin, Y., Han, G., 2024b. Effects of grazing and climate change on aboveground standing biomass and sheep live weight changes in the desert steppe in Inner Mongolia, China. Agricultural Systems 217, 103916. https://doi.org/10.1016/j.agsy.2024.103916.

Wen, P., Wei, Q., Zheng, L., Rui, Z., Niu, M., Gao, C., Guan, X., Wang, T., Xiong, S., 2023. Adaptability of wheat to future climate change: effects of sowing date and sowing rate on wheat yield in three wheat production regions in the North China Plain. Sci. Total Environ. 165906 https://doi.org/10.1016/j.scitotenv.2023.165906.

Yang, C., Fraga, H., van Ieperen, W., Trindade, H., Santos, J.A., 2019. Effects of climate change and adaptation options on winter wheat yield under rainfed Mediterranean conditions in southern Portugal. Clim. Change 154, 159–178. https://doi.org/10.1007/s10584-019-02419-4.

Yasin, M., Ahmad, A., Khaliq, T., Habib-ur-Rahman, M., Niaz, S., Gaiser, T., Ghafoor, I., Hassan, H.S.U., Qasim, M., Hoogenboom, G., 2022. Climate change impact uncertainty assessment and adaptations for sustainable maize production using multi-crop and climate models. Environ. Sci. Pollut. Res. 1-22 https://doi.org/10.1007/s11356-021-17050-z.

Yu, Y., Yang, X., Guan, Z., Zhang, Q., Li, X., Gul, C., Xia, X., 2023. The impacts of temperature averages, variabilities and extremes on China's winter wheat yield and its changing rate. Environmental Research Communications 5, 071002. https://doi.org/10.1088/2515-7620/ace2a0.

Zhang, D., Liu, J., Li, D., Batchelor, W.D., Wu, D., Zhen, X., Ju, H., 2023a. Future climate change impacts on wheat grain yield and protein in the North China Region. Sci. Total Environ. 166147 https://doi.org/10.1016/j.scitotenv.2023.166147.

Zhang, Y., Liu, H., Qi, J., Feng, P., Zhang, X., Li Liu, D., Marek, G.W., Srinivasan, R., Chen, Y., 2023b. Assessing impacts of global climate change on water and food security in the black soil region of Northeast China using an improved SWAT-CO2 model. Sci. Total Environ. 857, 159482 https://doi.org/10.1016/j.scitotenv.2022.159482.

Zhou, B., Sun, X., Ge, J., Li, C., Ding, Z., Ma, S., Ma, W., Zhao, M., 2020. Wheat growth and grain yield responses to sowing date-associated variations in weather conditions. Agron. J. 112, 985–997. https://doi.org/10.1002/agj2.20122.